International Journal of Earth Sciences (2021) 110:467–485
https://doi.org/10.1007/s00531-020-01963-0

ORIGINAL PAPER

Geochemistry and Sm–Nd isotopic sources of Late Ediacaran siliciclastic series in the Ossa–Morena Complex: Iberian–Bohemian correlations

Esther Rojo-Pérez[1] · José M. Fuenlabrada[2] · Ulf Linnemann[3] · Ricardo Arenas[1] · Sonia Sánchez Martínez[1] · Rubén Díez Fernández[4] · Luis Miguel Martín Parra[4] · Jerónimo Matas[4] · Pilar Andonaegui[1] · Javier Fernández-Suárez[1]

Received: 6 April 2020 / Accepted: 10 November 2020 / Published online: 2 January 2021

Abstract

The Cadomian basement in central and southern Europe is composed by Ediacaran–Early Cambrian sequences that appear dismembered along the Variscan Orogen. These ancient series contain geochemical and isotopic keys related to their deposition in different basins located along the paleo margin of Gondwana. The southwest of Iberian Massif (Ossa–Morena Complex) contains an excellent representation of Cadomian basement. The oldest sedimentary succession of this region, the Serie Negra Group (c. 600–541 Ma), is composed by the Montemolín Formation which consists of metapelites, metagreywackes and abundant amphibolites; and the Tentudía Formation which consists of metagreywackes, black quartzites and metapelites. The whole-rock and Nd isotopic geochemistry of the Montemolín and Tentudía formations, are consistent with a deposition in a back-arc or fore-arc setting. Their Nd isotopic composition shows highly negative $\varepsilon Nd_{(t)}$ values in a range between − 6.9 and − 11.5, resulting in old Paleoproterozoic Nd model ages between 1.9 and 1.7 Ga. The Nd isotopic signatures obtained for the Cadomian basement in the Iberian Massif are almost identical to those obtained for equivalent sedimentary series in the Saxo-Thuringian Zone (Bohemian Massif), where Nd model ages range between 2 and 1.6 Ga. The limited variability of these Nd-T_{DM} ages suggests that the southwestern Iberian and North Bohemian series shared a common source during Ediacaran times, which would be located close to the periphery of the West African Craton. The Nd isotopic data considered herein provide solid evidence about the peri-Gondwanan location and correlation between the Cadomian basement of southwestern Iberia and North Bohemia.

Keywords Late Ediacaran series · Iberian massif · Bohemian massif · Nd isotope geochemistry · Variscan correlation · Peri-Gondwana paleogeography

✉ Esther Rojo-Pérez
e.rojo@ucm.es

José M. Fuenlabrada
jmfuenla@ucm.es

Ulf Linnemann
ulf.linnemann@senckenberg.de

Ricardo Arenas
rarenas@ucm.es

Sonia Sánchez Martínez
s.sanchez@geo.ucm.es

Rubén Díez Fernández
r.diez@igme.es

Luis Miguel Martín Parra
lm.martin@igme.es

Jerónimo Matas
j.matas@telefonica.net

Pilar Andonaegui
andonaeg@ucm.es

Javier Fernández-Suárez
jfsuarez@ucm.es

1 Departamento de Mineralogía y Petrología and Instituto de Geociencias (UCM, CSIC), Facultad de Geología, Universidad Complutense de Madrid, C/José Antonio Novais, no 2, 28040 Madrid, Spain

2 Unidad de Geocronología (CAI de Ciencias de la Tierra y Arqueometría), Universidad Complutense, 28040 Madrid, Spain

3 Museum Für Mineralogie Und Geologie, Senckenberg Naturhistorische Sammlungen Dresden, Königsbrücker Landstr. 159, 01109 Dresden, Germany

4 Instituto Geológico y Minero de España, 28760 Tres Cantos, Madrid, Spain

Introduction

The Variscan Orogen resulted from the Paleozoic convergence between Gondwana and Laurussia that culminated with the assembly of Pangea (Matte 2001; Arenas et al. 2016a; Díez Fernández et al. 2016). This orogen, which extends throughout central and western Europe, in parts of north and northwest of Morocco as well as in the Appalachian Mountains of northeastern America, contains the suture of the Rheic Ocean, other minor sutures, and sections of the thinned paleomargin of Gondwana, which hosted a long-lived (Avalonian–Cadomian) active magmatic arc (Dalziel 1997; Fuenlabrada et al. 2010; Pereira et al. 2012a, b; Albert et al. 2015; Andonaegui et al. 2016). Variscan deformation is penetrative and strong along the orogen, and Alpine overprinting affected some areas. Yet, the Bohemian Massif in Germany, the Central and Armorican massifs in France and Iberian Massif in Iberian peninsula (Fig. 1), contain well-preserved low-strain and low-grade Neoproterozoic to Early Paleozoic sedimentary series (Linnemann et al. 2000; Fernández-Suárez et al. 2002; Murphy et al. 2002; Pereira 2015). The correlation between the sedimentary series of these nowadays distant massifs, as well as improving the knowledge of the primary location of the paleobasins along the (North African) Gondwana margin, are being actively investigated through the study of paleofauna provinces and stratigraphic record, as well as provenance studies.

It is widely accepted that the Late Paleozoic Gondwana–Laurussia interplay produced a complex dismembering and juxtaposition of terranes as a result of their progressive collision. From a paleogeographic point of view, adjoining sections of the Gondwana margin dispersed along the Variscan Orogen should have an analogous sedimentary record between Late Ediacaran and Early Cambrian times. However, the common azoic nature of many of these series and the complex deformation associated with Variscan tectonics, make it difficult to recognize the primary configuration of the sedimentary series and to establish correlations between them. For this reason, valuable information can be obtained from whole-rock major and trace element and Nd isotopic geochemistry, combined with U–Pb radiometric ages and Hf systematics of detrital zircon (Fernández-Suárez et al. 2002; Linnemann and Romer 2002; Pereira et al. 2006, 2015; Linnemann et al. 2008; Fuenlabrada et al. 2020).

The Sm–Nd isotopic geochemistry of siliciclastic rocks provides an excellent approach to the average composition, provenance and isotopic sources of the materials which form the upper continental crust (McLennan et al. 1990; McLennan and Hemming 1992). In provenance studies, siliciclastic rocks may provide more significant information than the associated igneous rocks (granitoids), since the juvenile material that may be involved in the generation of many igneous rocks can be mixed with older initial

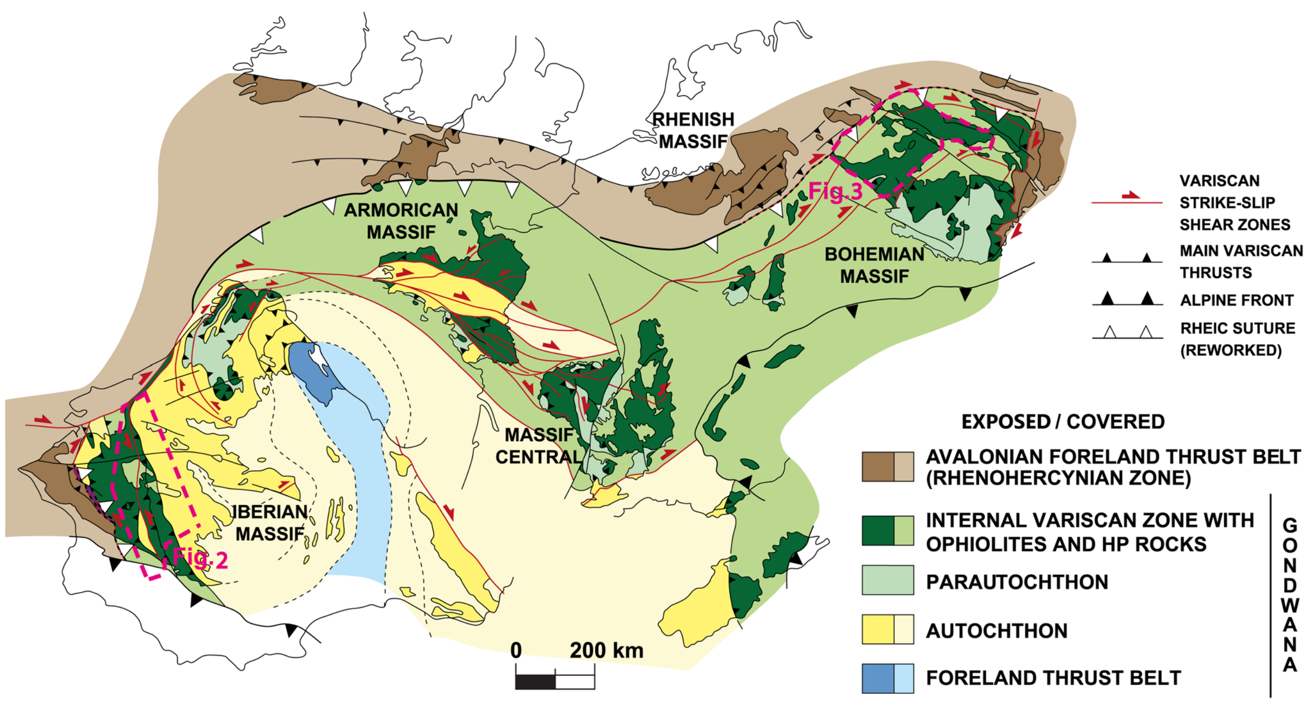

Fig. 1 Zonation of the European Variscan Orogen (Díez Fernández and Arenas 2015). Based on Franke (1989), and Martínez Catalán (2011). Location of Figs. 2 and 3 is shown

isotopic sources. This methodology has been scarcely used to investigate the provenance of the azoic series involved in the Variscan Orogen, unlike the many published papers focused on U–Pb geochronology of detrital zircon grains (e.g., Fernández-Suárez et al. 2007; Abati et al. 2010). Only combined U–Pb–Hf data on detrital zircon can provide comparable results in this sense (Avigad et al. 2012; Morag et al. 2012).

In the Iberian Massif, whole-rock major and trace element geochemistry and Nd isotopic geochemistry of siliciclastic rocks have been used in recent studies to investigate the tectonic setting and provenance of the sedimentary series deposited during the Ediacaran–Cambrian transition (Ugidos et al. 2003; Pereira et al. 2006; Guijarro et al. 2008; Fernández-Suárez et al. 2014; Fuenlabrada et al. 2016, 2020). However, the possible correlations of these Ediacaran series along the Variscan Orogen, between the Iberian and Bohemian massifs, and based on geochemical grounds that analyse the rock as a whole have not been explored in detail. In this sense, this work will improve the knowledge of the oldest siliciclastic series described in the Iberian Massif, the so-called Serie Negra Group (Carvalhosa 1965), including a new whole-rock geochemical and Sm–Nd isotopic database. These data are compared with the available isotopic (Nd) data from equivalent series described in the Bohemian Massif (Linnemann and Romer 2002), with the aim of testing the affinity of their isotopic sources between the Ediacaran series from both currently distant regions. Such comparison may help to refine reconstructions for the paleobasins once located along the (North African) margin of Gondwana that are now (dismembered and) spread as disconnected individual blocks of Cadomian basement throughout central and western Europe (Stephan et al. 2019a, b).

Geological setting

In the SW Iberian Massif, the lower part of the stratigraphic record of the continental allochthons of the Ossa–Morena Complex (Díez Fernández and Arenas 2015; Arenas et al. 2016b; Fig. 2) is part of a Cadomian basement that encompasses rocks from Neoproterozoic to Early Cambrian age. The Serie Negra Group (Carvalhosa 1965) is composed by a succession of metapelites and metagreywackes, interbedded with metamafic rocks and some layers of calc-silicate rocks and black quartzites. The thickest exposures of the Serie Negra Group occur in three key areas along NW–SE trending regional structures. From north to south these areas are: the Obejo-Valsequillo Domain (Ordóñez-Casado 1998; Bandrés 2001), the Olivenza–Monesterio antiform (Eguiluz and Quesada 1980; Montero et al. 1999) (Fig. 2) and the Aracena-Almadén de la Plata region (Ábalos 1987). Metamorphism in the Serie Negra Group ranges between greenschists facies conditions and pervasive migmatization. Among these key areas, the Olivenza–Monesterio antiform contains the most complete and well-preserved cross section to the Serie Negra Group, which shows a thickness exceeding c. 3000 m (Eguíluz 1988). The core of this antiform contains three stratigraphic formations, which from older to younger are referred to as the Montemolín, Tentudía and Malcocinado formations. Montemolín and Tentudía formations are traditionally considered to be two members of the Serie Negra Group. The c. 1000 m thick Montemolín Formation consists of metapelites, mica schists, quartz-rich schists, metagreywackes, metasandstones, abundant amphibolites (Sánchez-Lorda et al. 2013, 2016) toward the top and interbedded black quartzites. This formation may show extensive migmatisation towards the bottom (Montero et al. 1999). The Tentudía Formation is composed of metasandstones, metagreywackes, slates, phyllites, metacherts, black quartzites, layers of marble and micaschists. The overlying unconformable volcaniclastic Malcocinado Formation (Fricke 1941; Eguíluz et al. 2000) is composed by metaconglomerates, metasandstones, metapelites, meta-andesites and meta-rhyolites. The Serie Negra Group together with the Malcocinado Formation are unconformably covered by the Early Cambrian Torreárboles Formation (Liñán and Fernández-Carrasco 1984), composed by fluvial to shallow marine deposits with conglomerates, metasandstones and slates (Fig. 2).

A maximum depositional age of c. 565–541 Ma has been obtained for the Tentudía Formation using detrital zircon grains (Schäfer et al. 1993; Casado 1998; Linnemann et al. 2008). The Malcocinado Formation probably straddles the Ediacaran–Cambrian boundary (Pereira 2015). The Torreárboles Formation is Early Cambrian (Liñán and Fernández-Carrasco 1984), with a maximum depositional age of c. 540–532 Ma (Eguíluz 1988; Perejón et al. 2004; Pereira et al. 2011). Large massifs of igneous rocks, mainly of granitic–tonalitic composition, intruded into the Serie Negra Group between c. 600 and 540 Ma (Ordóñez-Casado 1998; Sánchez-García et al. 2003; Linnemann et al. 2008; Alvaro et al. 2014). This Ediacaran igneous suite was generated in relation to the prominent Avalonian–Cadomian peri-Gondwanan magmatic arc (Sánchez-García et al. 2013; Albert et al. 2015; Andonaegui et al. 2016). The chronology of this igneous suite suggests an age of c. 600 Ma for the undated oldest levels of the Montemolín Formation. This chronology is also compatible with the relationship of the Serie Negra Group with the opening of a fore-arc or back-arc basin in the peri-Gondwanan realm and the generation of associated supra-subduction zone type oceanic lithosphere (Arenas et al. 2018).

A similar Cadomian basement is widely exposed in other sections of the Variscan Orogen. In the eastern branch of the orogen, in the northern part of the Bohemian Massif (Fig. 3),

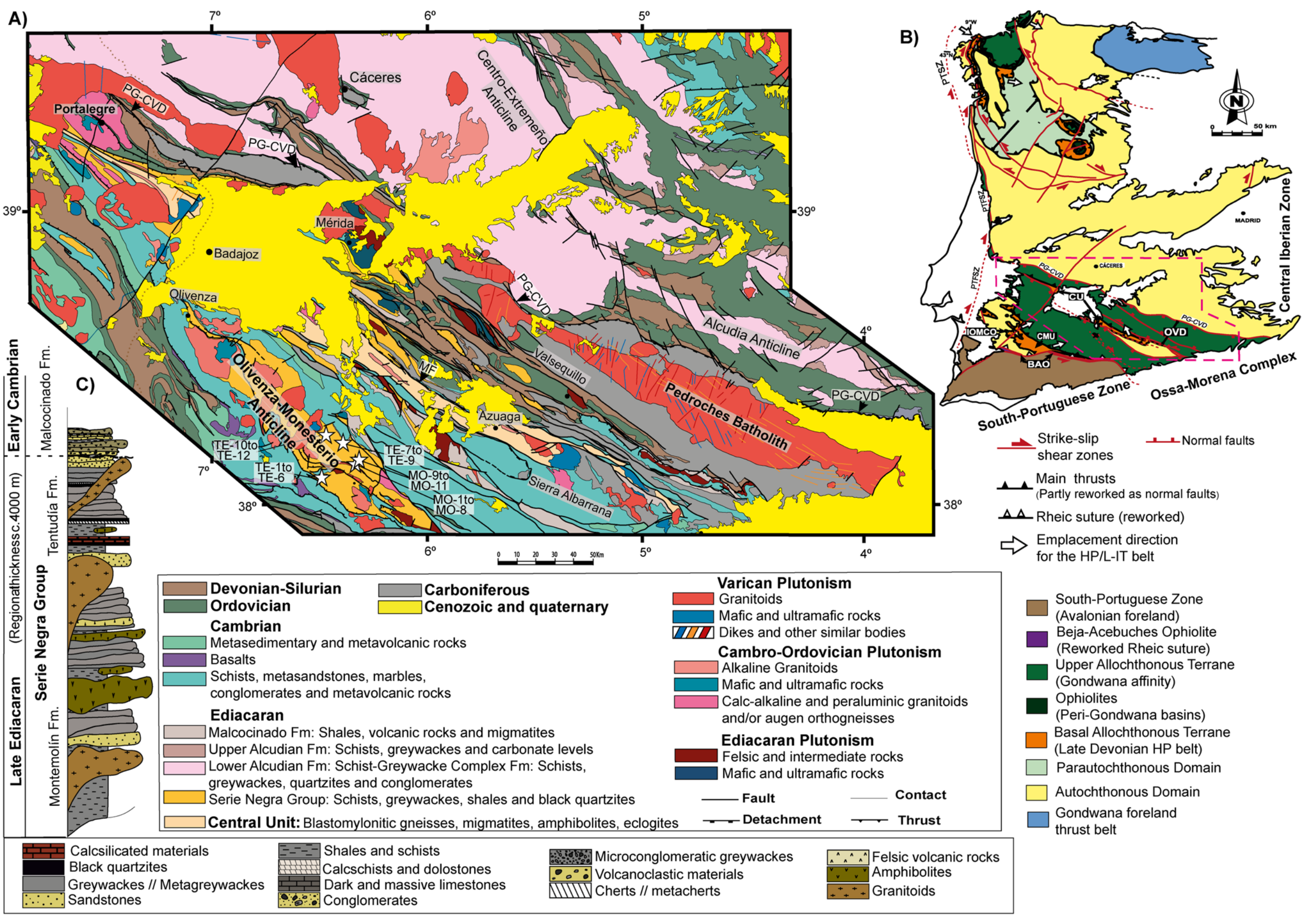

Fig. 2 **a** Geological map of the Ossa–Morena Complex including the south part of the Central Iberian Zone. Based on the 1:1.000.000 geological map of Spain and Portugal (IGME 2014; Rojo-Pérez et al. 2019). **b** Geological map of the Iberian Massif showing the distribution of allochthonous terranes in NW and SW Iberia (Díez Fernández and Arenas 2015). *BAO* Beja-Acebuches Ophiolite, *CMU* Cubito-Moura Unit, *CU* central unit, *IOMCO* Internal Ossa-Morena Complex Ophiolites, *OVD* Obejo-Valsequillo Domain, *PG–CVD* Puente Génave-Castelo de Vide Detachment, *PTSZ* Porto-Tomar Shear Zone. **c** Schematic stratigraphic column of the Serie Negra Group. TE and MO stars represent the sampling locations within the Olivenza–Monesterio Antiform

the Saxo-Thuringian Zone (SXTZ, Kossmat 1927) contains several Cadomian stratigraphic sequences with scarce Variscan overprint (Linnemann and Buschmann 1995), and probably equivalent to the Serie Negra Group (Pereira et al. 2006; Linnemann et al. 2008). The main outcrops are distributed along the northern margin of the SXTZ (Fig. 3), constituting a total of six siliciclastic series composed essentially by turbiditic metagreywackes, slates, phyllites, schists, metamafic rocks, black metacherts and some layers of quartzites and metaconglomerates toward the upper part of some formations. The oldest maximum depositional age for these formations is considered at c. 629 Ma, according to the U–Pb zircon dating of a granite pebble (Frohnberg Formation; Linneman et al. 2000). Moreover, a minimum depositional age at c. 543 Ma has been estimated using detrital zircon grains extracted from greywacke turbidites and a glaciomarine tillite (Linnemann et al. 2008, 2014, 2018). All these SXTZ formations are intruded by Ediacaran and Cambrian granitic rocks, with ages ranging between c. 540 and 537 Ma (Linnemann et al. 2000, 2010a, 2014, 2018). The Paleozoic sequence overlaying these Neoproterozoic series contains incomplete Cambro-Ordovician series and a more complete stratigraphic succession reaching the Lower Carboniferous (Brause 1968; Linnemann et al. 2010b).

Sample selection and methodology

Sample selection

Twenty-two samples of siliciclastic rocks belonging to the Serie Negra Group were collected in the Olivenza–Monesterio antiform. Ten samples belong to the Montemolín Formation (MO-1 to MO-11) and were collected in the northern

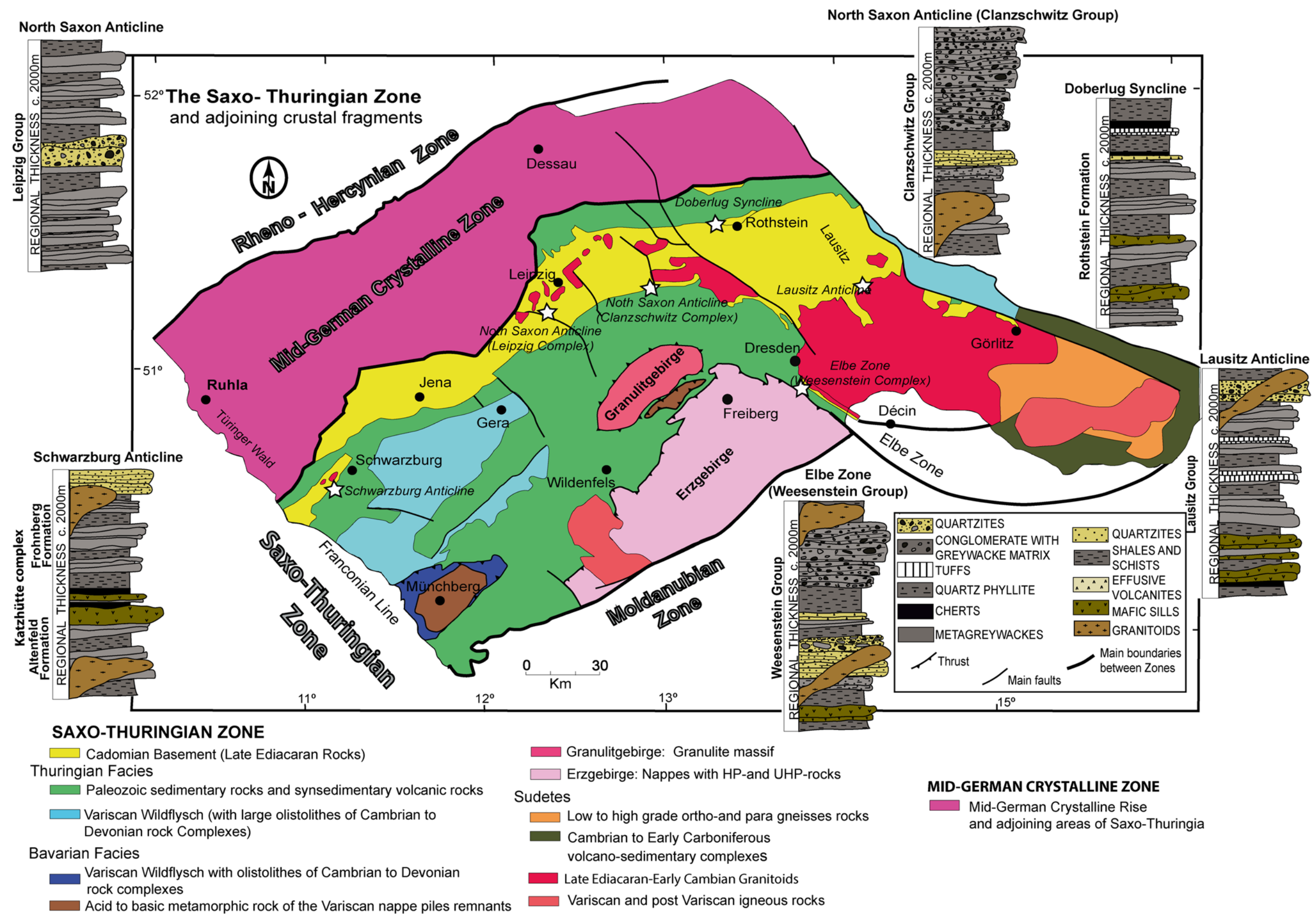

Fig. 3 Geological sketch of the Saxo-Thuringian Zone in the Bohemian Massif, including a schematic stratigraphic columns of the Ediacaran–Lower Cambrian series. Stars represent the location of the metasedimentary series. Based on Linnemann and Schauer (1999), Linnemann and Romer (2002) and Linnemann (2007)

limb of the antiform (Fig. 2). Each sample was extracted from an individual layer of metagreywacke (dm-scale in thickness). The remaining twelve samples belong to the Tentudía Formation (TE-1 to TE-12). They are predominantly fine-grained metagreywackes collected from individual layers and in equivalent proportions in both limbs of the Olivenza–Monesterio antiform (Fig. 2). All rocks sampled are fresh, without evidence of significant alteration. The outcrops visited during sampling indicate that the metasedimentary rocks sampled in the Montemolín Formation seem to accumulate more deformation (strain) than those collected in the Tentudía Formation, although collectively, all of the samples show low-grade metamorphism and slight to moderate strain. Yet, sampling was targeted to the sections with lowest strain.

In thin section, Montemolín samples show abundant micaceous minerals, including muscovite, biotite and chlorite, along with low deformed quartz-feldspathic levels. The samples exhibit heterogeneity in quartz and feldspar grain size, indicative of textural immaturity. This formation presents primary or tectonometamorphic compositional layering. On the other hand, in the Tentudía samples phyllosilicates are even more abundant, as well as opaque minerals and rock fragments. In general, these samples present a smaller grain size than Montemolín Formation and show higher plagioclase content in relation to K-feldspar.

Whole-rock major and trace elements analysis

Crushing and powdering of the rock samples were performed at the facilities of the Complutense University of Madrid. The analysis of major and trace elements were carried out in the Activation Laboratories (ActLabs), Ontario (Canada). Lithium metaborate/tetraborate was used for fusion of the samples, and the elements were measured by Inductively Coupled Plasma Mass Spectrometry (ICP-MS). The general precision was calculated at ~ 0.01%, and for MnO and Ti_2O at ~ 0.001%. The elemental composition of the Ediacaran metagreywackes was analysed to constrain their provenance and isotopic sources. The results of the

Table 1 Whole major and trace element data of Montemolín Formation (Late Ediacaran)

Sample	MO-01	MO-02	MO-03	MO-04	MO-05	MO-07	MO-08	MO-09	MO-10	MO-11
SiO_2	67.00	66.57	66.36	67.10	63.23	63.83	64.75	63.48	62.94	65.78
TiO_2	0.69	0.69	0.67	0.68	0.80	0.74	0.73	0.84	0.86	0.79
Al_2O_3	15.45	14.99	15.70	14.93	16.88	16.72	15.68	15.74	16.15	15.28
$Fe_2O_{3(T)}$	4.90	4.98	4.90	4.76	6.16	6.03	5.57	6.62	6.77	6.23
MnO	0.07	0.07	0.09	0.08	0.06	0.08	0.08	0.07	0.06	0.07
MgO	2.08	2.00	2.01	1.90	2.43	2.59	2.52	2.89	2.94	2.71
CaO	2.47	2.41	1.88	2.27	1.17	1.83	2.07	1.90	1.68	1.61
Na_2O	3.78	3.70	2.73	3.27	2.04	3.10	3.73	3.67	3.39	3.40
K_2O	2.21	2.10	2.94	2.24	4.20	3.36	2.51	2.84	2.96	2.47
P_2O_5	0.17	0.18	0.18	0.18	0.21	0.17	0.19	0.18	0.18	0.19
LOI	1.01	0.94	1.47	1.28	2.75	1.51	1.35	1.57	2.03	1.80
Total	99.83	98.63	98.94	98.68	99.92	99.96	99.19	99.80	99.96	100.33
PIA	67.93	67.84	73.46	69.61	79.80	73.05	69.43	69.84	72.23	71.89
CIA	59.45	59.48	62.15	60.67	63.17	60.58	59.15	58.21	59.55	59.99
SiO_2/Al_2O_3	4.34	4.44	4.23	4.49	3.75	3.82	4.13	4.03	3.90	4.30
K_2O/Na_2O	0.58	0.57	1.08	0.69	2.06	1.08	0.67	0.77	0.87	0.73
Al_2O_3/Na_2O	4.09	4.05	5.75	4.57	8.27	5.39	4.20	4.29	4.76	4.49
Al_2O_3/TiO_2	22.49	21.82	23.33	22.12	21.23	22.53	21.42	18.78	18.82	19.27
Ba	754	578	1009	876	1420	822	522	762	825	713
Rb	77	75	80	70	108	106	87	94	89	77
Sr	377	420	267	322	174	232	271	320	256	243
Nb	8.50	8.80	7.70	8.40	10.80	10.20	9.50	10.50	12.00	10.20
Hf	4.80	5.50	4.10	5.00	4.50	4.30	3.50	4.60	4.90	4.70
Zr	221	233	180	229	187	180	149	191	203	195
Y	21.70	22.00	21.50	21.00	23.40	23.10	22.50	23.00	25.60	23.50
Pb	24	21	18	24	18	20	22	15	18	20
Th	8.13	9.20	7.33	9.24	8.33	7.94	6.40	7.68	8.88	7.72
U	1.78	1.73	1.84	1.87	1.70	1.66	1.79	1.71	2.05	1.73
Cr	80	80	80	80	90	90	90	100	100	90
Ni	30	30	40	30	50	40	40	50	60	50
Co	14	14	16	14	16	17	15	21	23	24
V	91	89	111	89	120	106	105	118	123	114
Sc	11	11	12	11	16	14	13	15	16	15
Ga	19	17	19	18	21	20	20	20	23	20
Ti	4119	4119	4035	4047	4766	4448	4388	5024	5144	4754
Th/Nb	0.96	1.05	0.95	1.10	0.77	0.78	0.67	0.73	0.74	0.76
Th/Sc	0.74	0.84	0.61	0.84	0.52	0.57	0.49	0.51	0.56	0.51
La/Th	4.26	4.40	4.52	3.97	3.75	4.38	4.55	4.17	4.39	4.51
Zr/Sc	20.09	21.18	15.00	20.82	11.69	12.86	11.46	12.73	12.69	13.00
Ti/Zr	18.64	17.68	22.41	17.67	25.49	24.71	29.45	26.30	25.34	24.38
La	34.6	40.5	33.1	36.7	31.2	34.8	29.1	32	39	34.8
Ce	69.2	72.1	72.1	70.3	57.5	66	56.7	64.5	78.1	71.1
Pr	7.63	8.91	7.56	8.09	7.28	7.73	6.75	7.35	8.72	8.01
Nd	27.8	31.6	27.5	28.8	27.1	28.6	25.6	27	32.1	29
Sm	5.31	5.74	5.07	5.37	5.47	5.55	5.12	5.38	6.11	5.47
Eu	1.34	1.4	1.26	1.32	1.29	1.32	1.28	1.31	1.46	1.31
Gd	4.23	4.61	4.29	4.2	4.53	4.57	4.26	4.36	4.84	4.6
Tb	0.67	0.66	0.65	0.65	0.71	0.68	0.7	0.68	0.74	0.73
Dy	3.93	4.08	3.79	3.56	4.13	4.09	3.95	3.98	4.37	4.19
Ho	0.73	0.77	0.72	0.7	0.8	0.77	0.74	0.75	0.87	0.81
Er	2.1	2.15	2.12	2.09	2.38	2.23	2.16	2.2	2.5	2.27

Table 1 (continued)

Sample	MO-01	MO-02	MO-03	MO-04	MO-05	MO-07	MO-08	MO-09	MO-10	MO-11
Tm	0.30	0.32	0.31	0.29	0.35	0.31	0.31	0.32	0.36	0.32
Yb	2.04	2.1	2.1	2.04	2.33	2.24	2.09	2.21	2.43	2.13
Lu	0.32	0.32	0.31	0.32	0.35	0.35	0.32	0.34	0.38	0.33
ΣREE	160.21	175.27	160.89	164.44	145.43	159.25	139.09	152.38	181.99	165.08
Eu/Eu*	0.87	0.84	0.83	0.85	0.80	0.81	0.84	0.83	0.83	0.80
La_N/Yb_N	11.34	12.90	10.54	12.03	8.95	10.39	9.31	9.68	10.73	10.93
Gd_N/Yb_N	1.65	1.75	1.63	1.64	1.55	1.63	1.62	1.57	1.59	1.72
sumREE	160.21	175.27	160.89	164.44	145.43	159.25	139.09	152.38	181.99	165.08
LREE	318.02	357.47	314.78	331.16	290.49	317.97	274.96	301.34	361.34	326.55
HREE	76.99	80.01	76.91	74.68	84.35	81.26	78.64	79.82	88.96	83.04
LREE/HREE	4.13	4.47	4.09	4.43	3.44	3.91	3.50	3.78	4.06	3.93
La_N/Sm_N	4.02	4.35	4.03	4.22	3.52	3.87	3.51	3.67	3.94	3.93

analyses are included in Tables 1 and 2 and in the diagrams shown in Figs. 4, 5 and 7.

Whole-rock Sm–Nd isotopic analysis

Sm–Nd isotope analyses were performed using Isotope Dilution Thermal Ionization Mass Spectrometry (ID-TIMS) at the Geochronology and Isotope Geochemistry Facility of the Universidad Complutense de Madrid. Samples were spiked with a mixed ^{149}Sm-^{150}Nd tracer and then analysed in an IsotopX–Phoenix mass spectrometer (TIMS), following a single collection and a dynamic multicollection mode for Sm and Nd, respectively. To correct procedural and instrumental mass fractionation, the resulting $^{143}Nd/^{144}Nd$ ratios were corrected for ^{142}Ce and ^{144}Sm interferences and normalized to $^{146}Nd/^{144}Nd = 07219$ value (O'Nions et al. 1979). To have control over the drifts from La Jolla reference value (Lugmair et al. 1983), this standard was analysed along with the samples, yielding an average value of $^{143}Nd/^{144}Nd = 0.511851$ for six replicates, with an internal precision of ± 0.000007 (2σ). The analytical error for the $^{147}Sm/^{144}Nd$ and $^{143}Nd/^{144}Nd$ ratios was estimated lower than 0.1% and 0.006%, respectively, and Nd procedural blanks were always under 0.1 ng. The results are included in Table 3 and plotted on the diagram in Figs. 6, 7 and 8.

Whole-rock and isotope geochemistry results

The geochemistry of major elements in siliciclastic rocks is used to describe and constrain their nature and degree of alteration, as well as to characterize their provenance and tectonic setting during sedimentation (Nesbitt and Young 1982; Bhatia 1983; Taylor and McLennan 1985; Bhatia and Crook 1986). The use of immobile trace elements such as REE, Th, Co; Cr, Nb, Ti, Sc, Y, Zr, Hf, and especially their ratios, are excellent proxies to infer the likely tectonic setting and discriminate between felsic/mafic contributions from the source area, since they remain virtually undisturbed through weathering, transport, sedimentation and metamorphic processes (Nesbitt et al. 1980; Taylor and McLennan 1985; Wronkiewicz and Condie 1987; Feng and Kerrich 1990). The distribution of REE in detrital rocks reflects the average composition of the source area and, consequently, the REE-patterns are a means to discriminate between a crustal or mantle influence in the source. In this sense, certain crustal models consider Nd model age of siliciclastic rocks as an approximation to the average resulting of the extraction of the different terrigenous components from the melt source (McCulloch and Wasserburg 1978 and others), so Nd model ages may act as tracers of the crustal/mantle evolution of the detritus reaching a particular sedimentary basin (McLennan et al. 1990; McLennan and Hemming 1992).

Composition, classification and tectonic setting

The Montemolín and Tentudía formations define homogeneous series considering their major element composition (Tables 1 and 2). The SiO_2 average content for both formations (65.10 and 66.23 wt%, respectively) are slightly lower than the average described by Condie (1993) for the Upper Continental Crust (UCC) (66.79 wt%), while the average value for Fe_2O_3 (5.69 and 5.10 wt%, respectively) and Al_2O_3 (15.75 and 15.41 wt%, respectively) are slightly higher than typical UCC values (4.51 and 14.99 wt%, respectively). In both Montemolín and Tentudía formations, the mobile elements K_2O (avg. 2.78 and 2.59 wt%, respectively) and Na_2O (avg. 3.23 and 3.21 wt%) have an average content similar to the UCC range (3.1 and 3.35 wt%, respectively); only two samples (TE-03 and TE-10) show enriched and depleted contents, respectively, for these two elements compared to the average values of the group (Tables 1 and 2). The most significant difference between both Montemolín and

Table 2 Whole major and trace element data of Tentudía Formation (Late Ediacaran)

Sample	TE-01	TE-02	TE-03	TE-04	TE-05	TE-06	TE-07	TE-08	TE-09	TE-10	TE-11	TE-12
SiO_2	62.19	62.90	65.36	69.50	68.81	69.08	65.20	64.70	65.97	67.27	67.60	66.14
TiO_2	0.79	0.75	0.79	0.80	0.52	0.72	0.72	0.71	0.77	0.81	0.69	0.73
Al_2O_3	17.49	16.35	16.91	13.31	14.97	13.24	15.12	15.35	15.02	17.09	14.65	15.40
$Fe_2O_{3(T)}$	5.84	5.87	5.14	4.61	4.20	4.93	5.87	5.85	5.88	4.23	4.99	3.84
MnO	0.04	0.06	0.04	0.04	0.02	0.06	0.10	0.07	0.08	0.05	0.08	0.03
MgO	2.29	2.20	2.30	1.57	1.51	1.74	3.46	4.51	3.84	1.61	1.65	2.01
CaO	0.42	0.52	0.23	0.77	0.37	0.39	1.23	0.57	0.69	0.40	1.34	1.79
Na_2O	3.08	2.87	0.10	2.75	3.35	2.45	3.72	3.38	4.11	0.14	3.39	3.36
K_2O	2.47	2.84	4.87	1.95	2.17	2.17	1.66	1.66	1.19	5.23	2.44	2.47
P_2O_5	0.15	0.21	0.17	0.22	0.13	0.20	0.19	0.22	0.23	0.25	0.22	0.22
LOI	5.01	4.46	4.40	3.34	3.22	3.62	2.14	2.69	2.44	3.22	2.80	3.41
Total	99.77	99.02	100.31	98.85	99.27	98.60	99.41	99.71	100.22	100.30	99.85	99.41
PIA	81.10	79.94	97.33	76.34	77.48	79.58	73.11	77.61	74.24	95.65	72.08	71.52
CIA	67.92	65.98	69.27	65.41	66.92	66.23	60.02	60.27	60.44	69.84	62.42	61.53
SiO_2/Al_2O_3	3.56	3.85	3.87	5.22	4.60	5.22	4.31	4.21	4.39	3.94	4.61	4.29
K_2O/Na_2O	0.80	0.99	48.70	0.71	0.65	0.89	0.45	0.49	0.29	37.36	0.72	0.74
Al_2O_3/Na_2O	5.68	5.70	169.10	4.84	4.47	5.40	4.06	4.54	3.65	122.07	4.32	4.58
Al_2O_3/TiO_2	22.20	21.89	21.35	16.74	28.79	18.47	21.00	21.71	19.56	21.18	21.29	21.04
Ba	354	341	534	243	379	266	447	364	211	405	320	302
Rb	83	101	141	68	75	91	52	50	39	138	80	73
Sr	97	89	18	71	83	66	163	95	144	30	154	132
Nb	10.20	10.30	10.70	9.10	6.40	8.50	10.30	10.40	10.60	11.60	9.80	10.20
Hf	3.80	4.00	5.70	5.80	3.30	5.40	5.20	6.30	6.80	6.90	6.10	5.70
Zr	142	150	228	253	136	230	220	265	274	285	257	235
Y	26.90	25.40	21.40	24.10	15.50	21.90	21.30	22.70	23.10	23.10	26.00	25.50
Pb	5	5	5	62	7	5	8	5	6	5	6	5
Th	7.43	8.00	9.16	12.30	6.27	11.30	7.05	10.70	9.82	10.70	9.53	8.66
U	1.84	2.13	2.45	3.34	1.88	2.26	1.42	1.80	2.65	3.92	2.05	2.00
Cr	90	90	80	80	60	70	90	100	100	90	80	90
Ni	40	50	30	30	40	40	40	40	40	40	40	40
Co	11	13	13	10	11	13	19	19	19	21	16	15
V	127	122	103	85	73	81	92	101	105	97	90	94
Sc	17	16	13	11	10	10	12	13	13	13	11	12
Ga	21	22	22	16	17	16	20	20	20	22	19	20
Ti	4724	4478	4748	4766	3117	4298	4316	4238	4604	4838	4125	4388
Th/Nb	0.73	0.78	0.86	1.35	0.98	1.33	0.68	1.03	0.93	0.92	0.97	0.85
Th/Sc	0.44	0.50	0.70	1.12	0.63	1.13	0.59	0.82	0.76	0.82	0.87	0.72
La/Th	3.20	2.84	2.71	2.09	4.32	2.39	4.09	3.52	3.96	3.91	4.42	4.31
Zr/Sc	8.35	9.38	17.54	23.00	13.60	23.00	18.33	20.38	21.08	21.92	23.36	19.58
Ti/Zr	33.27	29.86	20.82	18.84	22.92	18.69	19.62	15.99	16.80	16.98	16.05	18.67
La	23.8	22.7	24.8	25.7	27.1	27	28.8	37.7	38.9	41.8	42.1	37.3
Ce	47.6	48.5	59	50.9	52.6	60.1	57.3	74.8	77.2	78.3	78.6	69.6
Pr	5.71	5.43	6.13	6.17	6.11	6.37	6.63	8.33	8.57	8.88	9.15	8.02
Nd	21.4	19.9	23.2	22.3	22.6	23	24.1	30.3	30.8	31.3	33	29.7
Sm	4.68	4.09	4.52	4.4	4.54	4.53	4.79	5.76	5.97	5.31	6.27	6.01
Eu	1.19	0.903	1.23	1.1	1.04	1.11	1.1	1.39	1.44	1.37	1.55	1.33
Gd	4.21	3.83	3.7	3.76	3.39	3.8	3.93	4.75	4.86	4.34	5.04	4.88
Tb	0.74	0.66	0.62	0.65	0.49	0.65	0.61	0.76	0.72	0.68	0.76	0.75
Dy	4.59	4.25	3.89	4.09	2.74	3.85	3.68	4.21	4.03	3.94	4.46	4.36
Ho	0.93	0.88	0.75	0.83	0.51	0.75	0.72	0.76	0.76	0.77	0.86	0.84

Table 2 (continued)

Sample	TE-01	TE-02	TE-03	TE-04	TE-05	TE-06	TE-07	TE-08	TE-09	TE-10	TE-11	TE-12
Er	2.73	2.52	2.15	2.48	1.49	2.22	2.01	2.17	2.28	2.32	2.39	2.4
Tm	0.40	0.39	0.34	0.37	0.22	0.33	0.30	0.33	0.33	0.34	0.34	0.36
Yb	2.68	2.56	2.25	2.51	1.44	2.17	1.98	2.17	2.17	2.39	2.42	2.39
Lu	0.41	0.37	0.34	0.38	0.23	0.33	0.31	0.32	0.33	0.38	0.33	0.36
ΣREE	121.08	116.99	132.93	125.64	124.50	136.21	136.26	173.75	178.36	182.12	187.27	168.31
Eu/Eu*	0.82	0.70	0.92	0.83	0.81	0.82	0.78	0.82	0.82	0.88	0.85	0.75
La_N/Yb_N	5.94	5.93	7.37	6.85	12.58	8.32	9.73	11.62	11.99	11.70	11.63	10.44
Gd_N/Yb_N	1.25	1.19	1.31	1.19	1.88	1.40	1.58	1.74	1.79	1.45	1.66	1.63
sumREE	121.08	116.99	132.93	125.64	124.50	136.21	136.26	173.75	178.36	182.12	187.27	168.31
LREE	230.98	221.29	253.14	244.35	251.37	262.74	269.84	345.80	356.03	366.11	376.89	336.18
HREE	91.31	84.95	76.63	82.41	56.15	76.98	73.08	83.53	83.03	81.67	89.00	88.26
LREE/HREE	2.53	2.60	3.30	2.97	4.48	3.41	3.69	4.14	4.29	4.48	4.23	3.81
La_N/Sm_N	3.14	3.42	3.39	3.60	3.68	3.68	3.71	4.04	4.02	4.86	4.14	3.83

Tentudía formations, in comparison with the UCC, appears in lower values of CaO content (1.93, 0.73 and 3.36 wt%, respectively). The higher amount of CaO in the Montemolín Formation than in the Tentudía Formation is likely linked with the occurrence within the Montemolín Formation of abundant mafic material (Montemolín amphibolites; Eguíluz et al. 1990). The average compositional ranges of TiO_2, MnO, MgO and P_2O_5 are 0.75 and 0.73 wt%; 0.07 and 0.06 wt%; 2.38 and 2.23 wt%; 0.18 and 0.20 wt%, for Montemolín and Tentudía rock samples, respectively.

Whole-rock anhydrous chemical compositions of the Montemolín and Tentudía samples have been plotted in the classification diagram published by Herron (1988; Fig. 4a). The rocks sampled in both formations appear at the outcrop as little deformed common greywackes. However, they exhibit a relative compositional heterogeneity when plotted in this classification diagram. A part of the Tentudía and the whole Montemolín samples appear represented into the shale field. This depiction, in the case of Montemolín Formation, seems motivated for their relatively low SiO_2 contents. While for Tentudía Formation, such plotting can be explained by its low K_2O values, which may reflect a significant post-depositional weathering characteristic of this element. It is appropriate to use other indexes and immobile ratios for accurate measuring of the maturity and weathering of these rocks.

The average values of the SiO_2/Al_2O_3, K_2O/Na_2O, Al_2O_3/Na_2O, Al_2O_3/TiO_2 ratios for the Montemolín Formation (4.14, 0.91, 4.99, and 21.18, respectively; Tables 1 and 2) show no significant deviation from those in the Tentudía Formation (4.34, 0.67, 4.73, and 21.27, respectively), falling within the range estimated by Condie (1993) for the UCC (4.46, 0.93, 4.47 and 24.18, respectively), which suggests an immature nature. The very low values of the K_2O/Na_2O and Al_2O_3/Na_2O ratios, with respect to the PAAS (Post Archean Australian Shale, Taylor and McLennan 1985), confirm this immaturity as well as a certain predominance of plagioclase over K-feldspar (except for the TE-03 and TE-10 samples) and white mica in the sedimentary protoliths. The limited effect of weathering processes and the immature character of the sedimentary protoliths from both formations are also supported by a negative correlation between the SiO_2 and the rest of major elements, which is reflected in the homogeneous and restricted major element variation of all the samples (Fig. 4b). The CIA (Chemical Index of Alteration; Nesbitt and Young 1982) and PIA (Plagioclase Index of Alteration; Fedo et al. 1995) values for the Tentudía Formation (avg. 63.71 and 76.30, respectively) are slightly higher than those of the Montemolín Formation (avg. 60.24 and 71.51, respectively), and lower than those of the PAAS (avg. 73.70 and 79.02, respectively). These values are consistent with a limited degree of post-depositional alteration and a scarce influence of the sedimentary transport over plagioclase and K-feldspar.

The REE chondrite-normalized fractionation patterns (Nakamura 1974) in Montemolín and Tentudía formations exhibit an enrichment of the LREE (avg. La_N/Sm_N: 3.90 and 3.79, respectively; Tables 1 and 2), and relatively flat patterns for the HREE, with Gd_N/Yb_N values close to unity (avg. 1.64 and 1.51, respectively). The metagreywacke samples from the Tentudía Formation display REE patterns (avg. La/Yb_N 9.51) closer to those of the PAAS (9.06), than samples of the Montemolín Formation (avg. La/Yb_N 10.68) (Fig. 4c). All the samples show slightly negative Eu anomalies, whose average values for the Montemolín and Tentudía formations are 0.83 and 0.82, respectively (Eu/Eu* calculated according to Taylor and McLennan 1985).

Trace elements such as La, Zr, Th, Nb, Sc, Y, Ti, and Co, as well as their ratios, are useful tectonic setting and provenance discriminators for (meta)sedimentary rocks

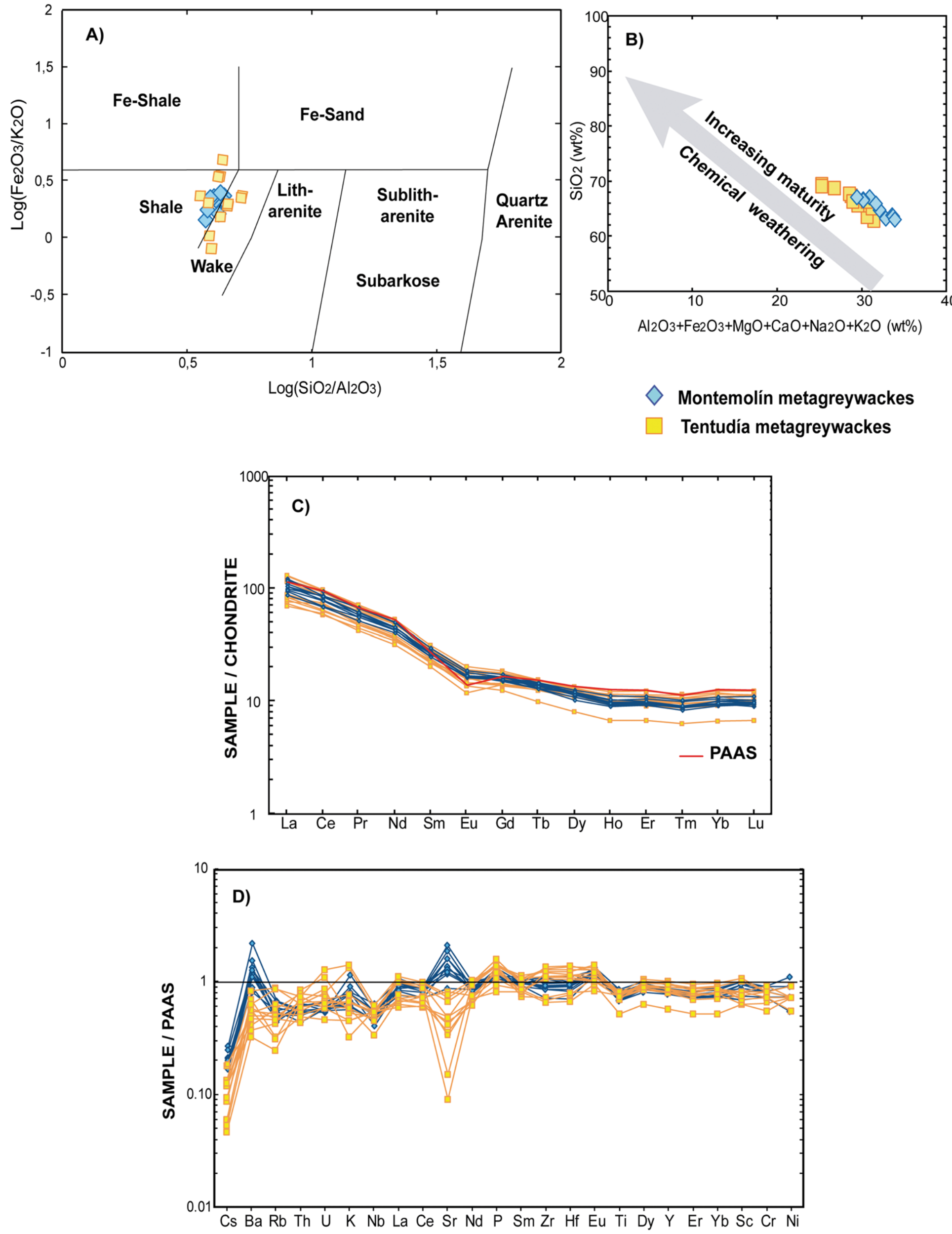

Fig. 4 Chemical diagrams for Montemolín and Tentudía formations. **a** Chemical classification diagram based on major elements (Herron 1988). **b** Maturity and chemical weathering diagram based on major element distribution (after Linnemann and Romer 2002). **c** Chondrite normalized REE plot (Nakamura 1974); red line corresponds to the PAAS (Post Archean Australian Shale; Taylor and McLennan 1985). **d** PAAS normalized trace elements diagram

(Bhatia and Crook 1986), since some of these elements are directly associated with felsic (Th y La) or mafic (Sc and Cr) sources. Th/Nb values for Montemolín and Tentudía formations (avg. 0.85 and 0.95, respectively; Tables 1 and 2) are slightly higher to those of PAAS (0.77), whereas the Th/Sc ratio obtained for the Montemolín Formation (0.62) is lower than Tentudía Formation and PAAS (0.76 and 0.91, respectively). A relative enrichment in Sc in the Montemolín Formation is in agreement with its CaO values. The average values in Montemolín and Tentudía formations for the La/Th (4.29, and 3.48, respectively) and Zr/Sc (15.15 and 18.29, respectively) ratios are higher than the estimated for the UCC and the PAAS (2.7 and 13.13, respectively). These values point to a mixed source, dominated by an intermediate-felsic component (Cullers 2002). This interpretation is also suggested by the low values observed in both formations in the Ti/Zr ratio (23.21 and 20.71, respectively); and low contents of Cr (avg. 88 and 85, respectively), and Ni (avg. 42 and 39, respectively).

A set of major and trace elements analyses (following Thompson 1982) was normalized to PAAS and plotted into a multivariate diagram for both Ediacaran metasedimentary series (Fig. 4d). Both formations display very similar patterns. They show depletion in the LILE elements, with larger variability in the metagreywackes from the Tentudía Formation, especially in K and Sr, probably due to some post-depositional alteration. Instead, the metagreywackes from Montemolín Formation show a

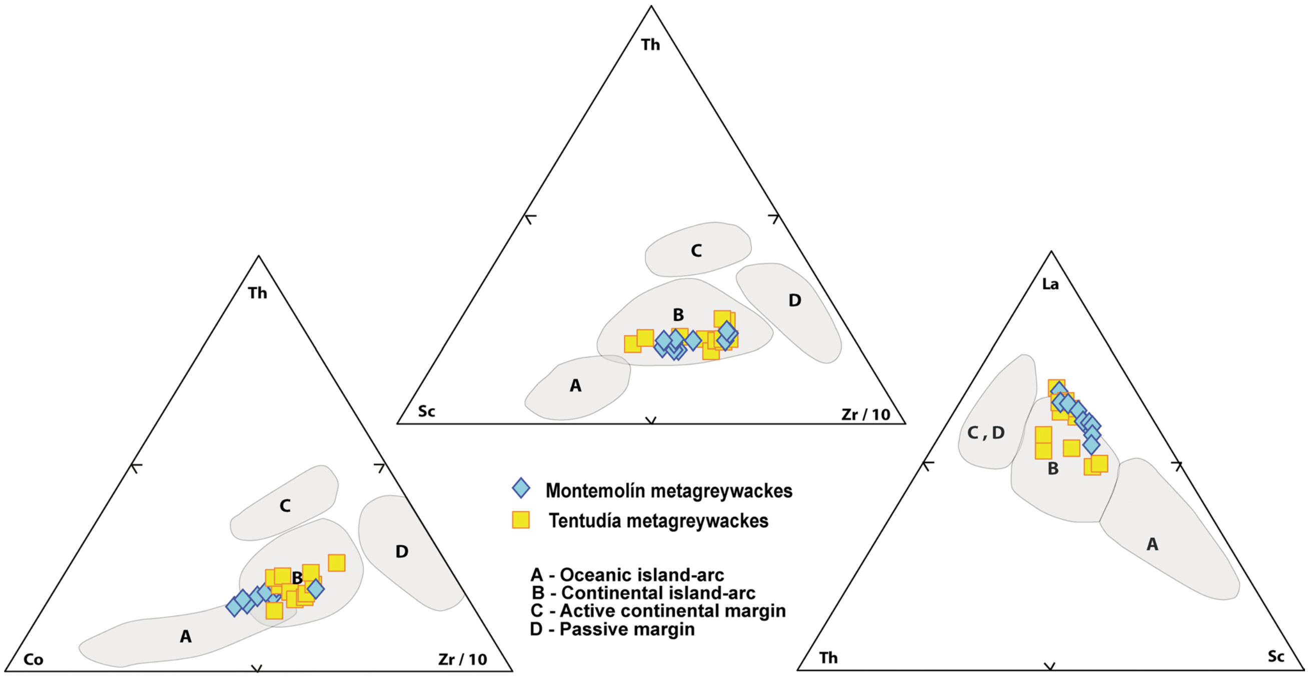

Fig. 5 Trace element diagrams with tectonic setting discrimination fields (after Bhatia and Crook 1986)

significant enrichment in Sr, linked to the high content in CaO described above. In both formations, LILE elements exhibit a slightly positive slope, while the HSFE element (Zr, Hf, Sm, HREE, and Sc) display flat patterns close to unity (Fig. 4d). A Ti negative anomaly is present in both formations, as expected for a dominant felsic provenance. The patterns of Montemolín and Tentudía formations are consistent with the features described for sediments deposited in an active margin setting (Winchester and Max 1989).

The Montemolín and Tentudía formations lack of large deviations of their geochemical composition from references such as PAAS and UCC. Low Na, Ca, K and Sr contents may indicate weak post-depositional weathering/recycling alteration, but with no significant consequences for using immobile trace elements on provenance and tectonic setting discrimination diagrams. Ternary diagrams (Bhatia and Crook 1986; La–Th–Sc, Th–Co–Zr/10 and Th–Sc–Zr/10) (Fig. 5) provide a valuable tool to distinguish between four depositional settings for sedimentary series. All samples plot into the same field (*B*), suggesting a similar geodynamic environment for their sedimentation during Ediacaran times (Fig. 5). This tectonic setting would be characterized by the presence of a magmatic arc, built over a thinned continental crust. The La/Sc ratios for both Ediacaran formations (2.65 and 2.58 for Montemolín and Tentudía Formations, respectively) close to the PAAS value (2.38; Taylor and McLennan 1985), and Ti/Zr ratios all above 20, strengthen the aforementioned geodynamic environment interpretation, since the values are close to the range for the continental island arc setting defined by Bhatia and Crook (1986).

Sm–Nd isotope geochemistry

To constrain the paleo-location of the basins where the Neoproterozoic sedimentary series were deposited, additional information to the major-trace element geochemical features is provided by the Sm–Nd system. These two elements are strongly immobile, thus reflecting an average of the original isotope composition from the mantle/crust source rocks. In this context, Nd model ages (T_{DM}) in siliciclastic rocks may be regarded as a proxy for the average age of extraction of their constituents from a depleted mantle, and therefore, the study of the Nd isotope composition of sedimentary sequences provides an excellent tool to understand crustal evolution (McCulloch and Wasserburg 1978; Allegre and Rousseau 1984; McLennan et al. 1990), as well as to constrain the mantle/crust provenance of terrigenous sediments.

Sm–Nd isotope data from the metagreywackes of the Tentudía and Montemolín formations are given in Table 3 and plotted in Fig. 6. Age assignment for the calculation of $\varepsilon Nd_{(T)}$ is based on the stratigraphic and structural features of the selected samples (see "Geological setting"). The reference depositional age considered for the Montemolín Formation (older part of the Ediacaran Serie Negra Group) is 600 Ma, and 565 Ma for the Tentudía Formation (upper part). The metagreywackes from Montemolín Formation show homogeneous $^{147}Sm/^{144}Nd$ ratios, which vary between

Table 3 Whole rock Nd isotope data of Montemolín and Tentudía Fms. (Late Ediacaran)

Sample	Sm	Nd	$^{147}Sm/^{144}Nd$	$f_{Sm/Nd}$	$^{143}Nd/^{144}Nd$	± StErr*10^{-6}	$\varepsilon Nd_{(0)}$	$\varepsilon Nd_{(T)}$ [a]	$T_{DM(Ma)}$ [b]
MO-1	4.95	26.78	0.1117	−0.432	0.511799	1	−16.4	−9.9	1859
MO-2	5.56	30.36	0.1106	−0.438	0.511764	1	−17.1	−10.5	1892
MO-3	5.25	27.59	0.1151	−0.415	0.511911	2	−14.2	−7.9	1747
MO-4	5.24	28.70	0.1104	−0.439	0.511792	1	−16.5	−9.9	1846
MO-5	5.10	26.21	0.1176	−0.402	0.511929	2	−13.8	−7.8	1765
MO-7	5.22	27.70	0.1138	−0.421	0.511863	1	−15.1	−8.8	1799
MO-8	4.79	24.32	0.1191	−0.395	0.511942	1	−13.6	−7.6	1772
MO-9	5.00	25.85	0.1168	−0.406	0.511860	1	−15.2	−9.1	1860
MO-10	5.79	31.04	0.1128	−0.426	0.511843	1	−15.5	−9.1	1811
MO-11	5.25	27.53	0.1154	−0.414	0.511902	1	−14.4	−8.1	1767
TE-01	4.26	19.88	0.1296	−0.341	0.512038	1	−11.7	−6.9	1819
TE-02	3.91	19.01	0.1242	−0.368	0.512012	1	−12.2	−7.0	1753
TE-03	4.43	22.46	0.1191	−0.395	0.511870	1	−15.0	−9.4	1889
TE-04	4.19	21.56	0.1175	−0.403	0.511832	1	−15.7	−10.0	1918
TE-05	3.91	20.75	0.1139	−0.421	0.511937	1	−13.7	−7.7	1686
TE-06	4.21	21.76	0.1168	−0.406	0.511827	1	−15.8	−10.1	1913
TE-07	4.46	22.95	0.1175	−0.403	0.511868	1	−15.0	−9.3	1861
TE-08	5.18	27.69	0.1130	−0.425	0.511789	1	−16.6	−10.5	1898
TE-09	5.60	29.84	0.1134	−0.424	0.511833	1	−15.7	−9.7	1837
TE-10	5.16	29.76	0.1049	−0.467	0.511711	1	−18.1	−11.5	1865
TE-11	5.88	31.79	0.1119	−0.431	0.511821	1	−15.9	−9.8	1828
TE-12	5.48	28.35	0.1169	−0.406	0.511836	1	−15.6	−9.9	1900

MO Montemolín Fm. of the Serie Negra (Ossa-Morena Complex), *TE* Tentudía Fm. of the Serie Negra (Ossa-Morena Complex)

[a] $\varepsilon Nd_{(T)}$ calculated for 600 and 565 Ma at the Montemolín and Tentudía Fm., respectively

[b] Nd model ages after DePaolo (1981)

Decay constant for ^{147}Sm: 6.54×10^{-12} years^{-1} (Lugmair and Marti 1978)

Present-day CHUR parameters: $^{147}Sm/^{144}Nd = 0.1967$; $^{143}Nd/^{144}Nd = 0.512638$ (Jacobsen and Wasserburg 1980)

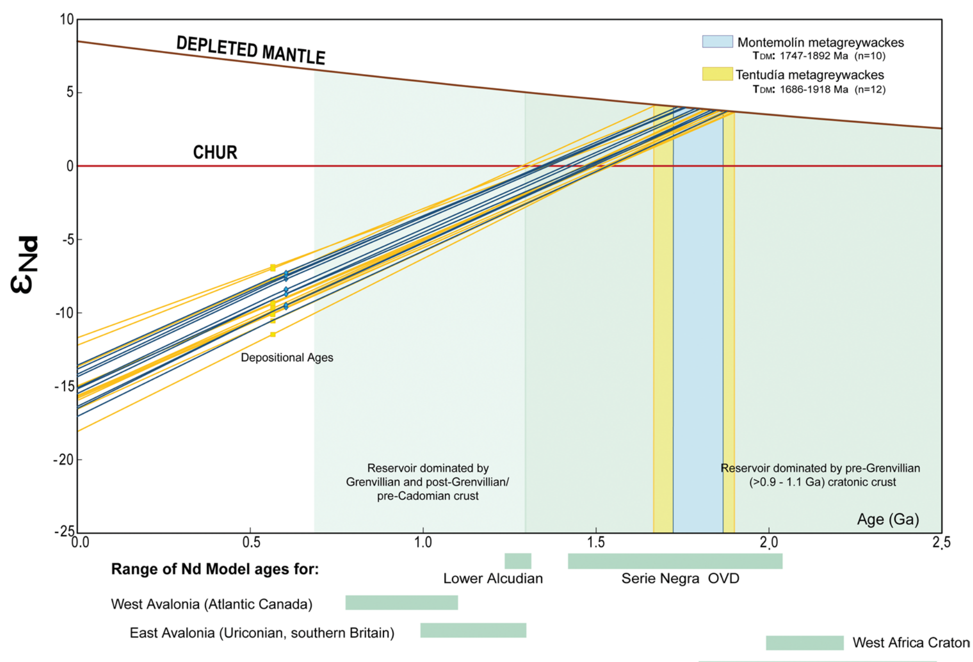

Fig. 6 εNd vs. age diagram showing T_{DM} values for the Late Ediacaran siliciclastic rocks of the Tentudía and Montemolín formations. The range of Nd model ages of selected regions are shown for comparison (Linnemann and Romer 2002; Fuenlabrada et al. 2016; Rojo-Pérez et al. 2019)

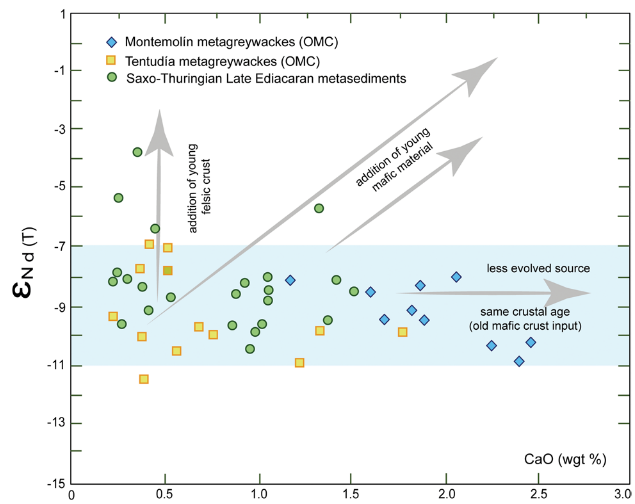

Fig. 7 $\varepsilon Nd_{(T)}$ vs. CaO diagram for Late Ediacaran series of the Ossa-Morena Complex (SW Iberian Massif) and the Saxo-Thuringian Zone (Bohemian Massif), showing the influence of young mafic or felsic contribution, or less evolved components (after Linnemann and Romer 2002). The blue band shows the range where the majority of samples plot

0.1104 and 0.1191, being very close to the value defined for the UCC (0.12), while the metagreywackes from Tentudía Formation display larger variability in $^{147}Sm/^{144}Nd$ ratios, ranging from 0.1049 to 0.1296. Both groups of ratios remain within the typical range established by Zhao et al (1992) for clastic sediments (0.1–0.13), and far from the upper limit suitable for Nd model ages calculation (0.165; Stern 2002). $f^{Sm/Nd}$ values represent the deviation of the $^{147}Sm/^{144}Nd$ ratios from the present CHUR values (Table 3). This factor calculated for the samples of the Montemolín Formation yields a very restricted value range (– 0.39 to – 0.44), reflecting a considerable isotopic homogenization. On the other hand, the metagreywackes from Tentudía Formation display a slightly wider range of values, varying from – 0.34 to – 0.47, which may suggest a lower influence of recycling processes.

All of the metagreywacke samples from both formations display very negative $\varepsilon Nd_{(0)}$ values, ranging between – 13.6 and – 17.1 for the Montemolín Formation; and between – 11.7 and – 18.1 for the Tentudía Formation. The $\varepsilon Nd_{(t)}$ follows a similar trend in both formations: metagreywackes from Montemolín Formation show an $\varepsilon Nd_{(600)}$ values ranging between – 7.6 and – 10.5, while in the metagreywackes from Tentudía Formation the $\varepsilon Nd_{(565)}$ ranges from – 6.9 to – 11.5. For the entire Serie Negra Group, these negative values together with the low ranges of the $f^{Sm/Nd}$ values are consistent with a provenance from old and recycled sources mixed with juvenile components (McLennan and Hemming 1992). The fact that both formations have such similar $\varepsilon Nd_{(t)}$ values suggests that their sources probably remained constant throughout the sedimentation period that encompasses both formations.

The calculated T_{DM} model ages for both formations of the Serie Negra Group plot within a restricted range of Paleoproterozoic ages (Fig. 6). The age vs. εNd diagram shows a clear overlap for both formations, with T_{DM} values varying from 1747 to 1892 Ma for the Montemolín Formation, and from 1686 to 1918 Ma in the Tentudía Formation. This figure also contains a synthesis of Nd model ages from the Serie Negra Group exposed in the Obejo-Valsequillo Domain (Rojo-Pérez et al. 2019), and from the Lower Alcudian section of the Central Iberian Zone (CIZ; Fuenlabrada et al. 2016), together with other Nd model ages from Central Europe (Linnemann and Romer 2002), are represented in Fig. for discussing paleogeographic affinities: old isotopic signatures from the West African Craton and the Amazonian Craton, conjoined with more juvenile ones such as those from West Avalonia in Atlantic Canada and Carolina.

Comparison with Central European correlatives: Saxo-Thuringian Zone series.

The affinity between Variscan sectors, which according to geotectonic and paleontological criteria share a common pre-Paleozoic evolution, has been studied and debated before (Murphy et al. 2002; von Raumer and Stampfli 2008; von Raumer et al. 2015; Ballèvre et al. 2014; Martínez Catalán et al. 2020). Nevertheless, geochemistry and especially isotopic approaches have not been extensively considered to correlate now distant, but potentially equivalent, metasedimentary sequences that made the Cadomian basement involved in the Variscan Orogen (Liew and Hofmann 1988; Pereira et al. 2006). This kind of comparison can help to understand Cadomian regions with low quality or lack of exposures and/or subjected to intense deformation and metamorphism. The new geochemical Sm–Nd isotopic data obtained herein for the Cadomian basement of the Ossa–Morena Complex, can be compared with equivalent coeval stratigraphic series described in the Cadomian basement of the Saxo-Thuringian Zone. Different Nd isotopic data from the Ediacaran series of the Bohemian Massif have been published (Linnemann and Romer 2002; Linnemann et al. 2004). From these data, only samples that can be considered lithologically comparable to those from SW Iberia have been used to perform a Nd isotopic comparison. These samples are mainly Late Ediacaran metagreywackes and metapelites and consist of a group composed by 23 samples. These siliciclastic rocks belong to four different units of the Bohemian Cadomian basement, which include the following successions: Frohnberg, Leipzig, Clanzschwitz and Rothstein formations; Lausitz and Weesenstein groups. Lithological details

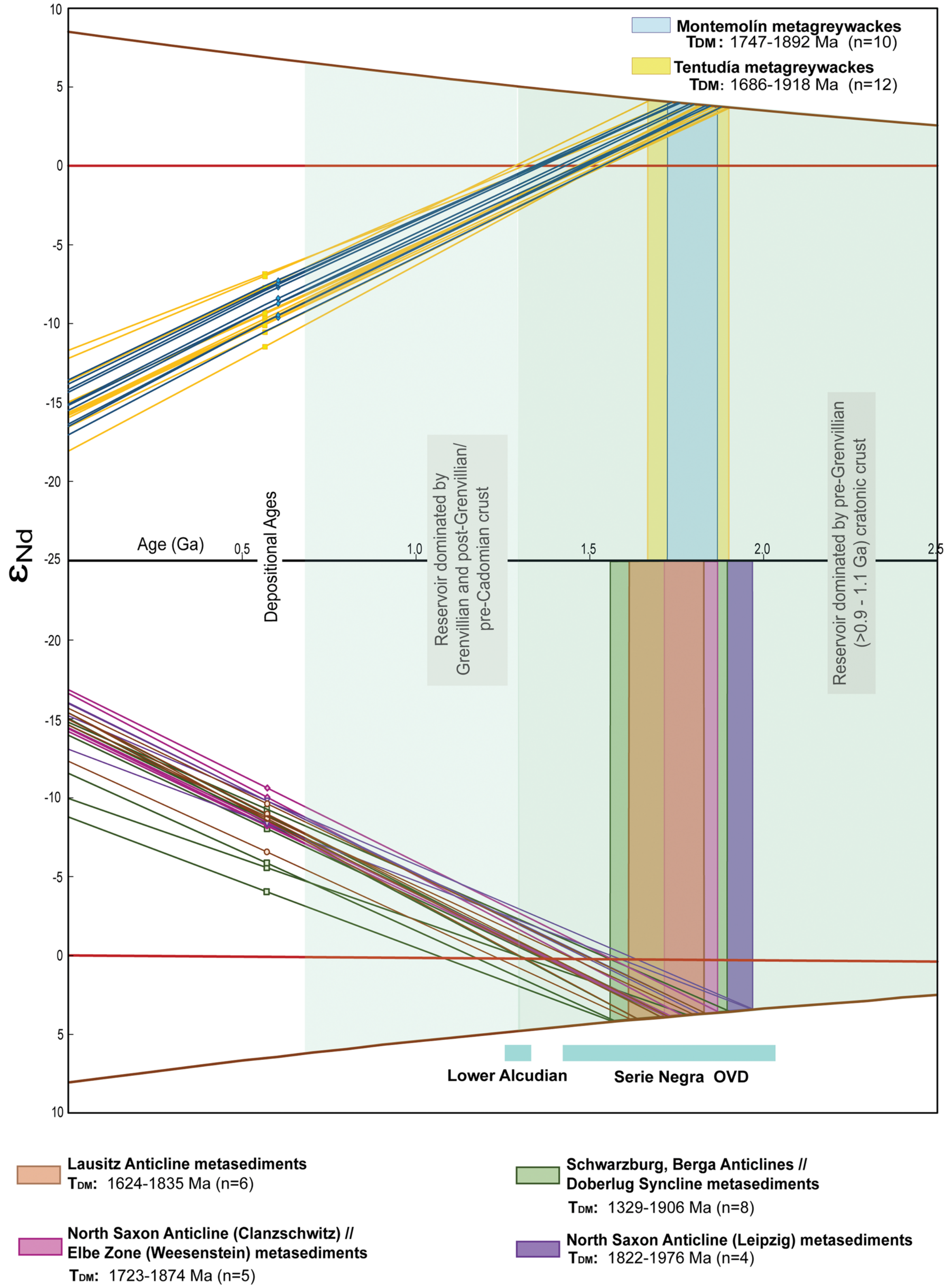

Fig. 8 εNd vs. age diagrams showing the T_{DM} values for the Tentudía and Montemolín Late Ediacaran series, compared with the Late Ediacaran series from the Saxo-Thuringian Zone. The ranges of Nd model ages of other coeval SW Iberian series (Fuenlabrada et al. 2016; Rojo-Pérez et al. 2019) are also plotted. Saxo-Thuringian data are extracted from Linnemann and Romer (2002)

of the Late Ediacaran series from Iberian and Bohemian massifs, and the number of rocks sampled in the different locations are presented in Figs. 2, 3 and 8.

The diagram CaO vs. $\varepsilon\mathrm{Nd}_{(T)}$ (Fig. 7) shows the influence of felsic or mafic (more juvenile) contributions in the siliciclastic rocks, as well as the contribution of old crustal areas. CaO contents in the Tentudía Formation show uniform distribution, similar to the distribution followed by the Saxo-Thuringian rocks, in both cases suggesting mixed felsic–mafic sources. However, the samples from the Montemolín Formation show a different trend directed toward less evolved source areas. The higher CaO values (avg. 1.93 wt%) are consistent with the presence of a significant volume of metamafic igneous rocks interbedded in this sequence. In Fig. 7, the Ediacaran samples show a wide variation in CaO with little changes in $\varepsilon\mathrm{Nd}_{(t)}$ values. Most samples fall into a restricted range of $\varepsilon\mathrm{Nd}_{(t)}$ values, ranging between − 7 and − 11 (Figs. 7 and 8). Three samples show less negative values of $\varepsilon\mathrm{Nd}_{(t)}$, probably due to the addition of juvenile material derived from an active magmatic arc. The homogeneous distribution, with little or no variation in $\varepsilon\mathrm{Nd}_{(t)}$, can be interpreted as evidence for a common isotopic source area, which should have remained available for a long time in the (North African) margin of Gondwana. This uniformity and availability are also reflected in the $\varepsilon\mathrm{Nd}_{(0)}$ values of the Bohemian series compared. Linnemann and Romer (2002) obtained highly negative $\varepsilon\mathrm{Nd}_{(0)}$ values for the SXTZ series, ranging between − 16.6 and − 12.8, except for the three samples mentioned above with larger juvenile input.

The εNd vs. time diagram presented in Fig. 8 shows a comparison between the isotopic composition of the SXTZ (North Bohemia) samples and the siliciclastic rocks of the Serie Negra Group. The Nd model ages obtained for the Bohemian samples define a relatively narrow age group ranging between 1570 and 1976 Ma. This age range is somewhat greater than that defined by the Montemolín and Tentudía formations of the Serie Negra Group. However, the two groups of samples are similar in relation to their isotopic sources, which very likely indicate a common source area for the North Bohemian and SW Iberian massifs during Ediacaran times. Their source area must have remained available at least during the depositional time of all the Ediacaran series. As a result, these data seem to indicate a common palaeographic context in the (North African) margin of Gondwana for the two regions. Ediacaran proto- North Bohemia and proto- SW Iberia were probably part of the same (or closely connected) sedimentary basin(s), where turbiditic siliciclastic series that shared common source areas were deposited (Fig. 9).

Discussion

In the southwest part of the Iberian Massif, the Ossa–Morena Complex represents the most external section of the Gondwana margin (Díez Fernández and Arenas 2015). This section and its prolongation in the allochthonous complexes of NW Iberia, was affected by an intense Variscan deformation

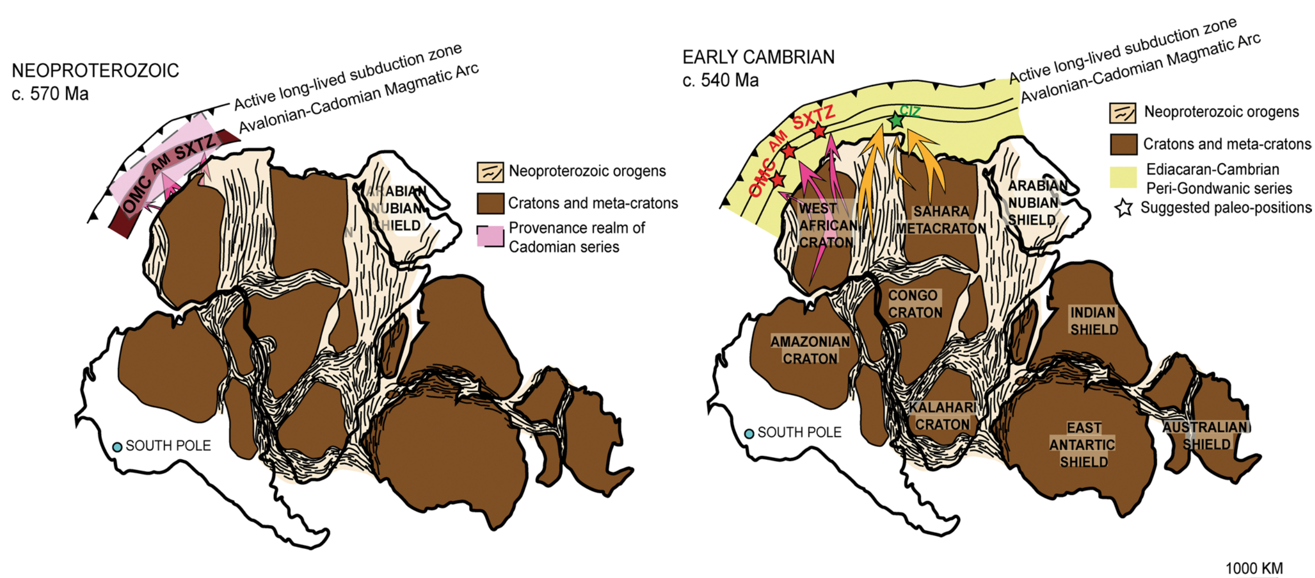

Fig. 9 Paleogeographic reconstruction at *c.* 570 and 540 Ma, showing the paleo-position inferred for the deposition of the Late Ediacaran series located in the Ossa-Morena Complex (OMC), Armorican Massif (AM), Saxo-Thuringian Zone (SXTZ) and Central Iberian Zone (CIZ) along the (North African) margin of Gondwana. The arrows indicate the location of the source areas and the direction of sediment transport into the peri-Gondwanan basin. Gondwana paleogeography based on von Raumer and Stampfli (2008), Meert and Bruce (2008) and Díez Fernández et al. (2010)

(Arenas et al. 2016a; Díez Fernández et al. 2016). The Variscan orogenic evolution resulted in an intricate amalgamation of terranes with different origin and tectonothermal evolution, which make it difficult to correlate units along the orogen. The (North African) margin of Gondwana has been interpreted as a long-lived magmatic arc, probably active in the period ranging between c. 750 and 500 Ma (Linnemann et al. 2004; Rodriguez-Alonso et al. 2004; Pereira et al. 2006, 2012b; Andonaegui et al. 2016). The activity of this magmatic arc can be tracked by both the related igneous rocks and through the sedimentary record generated during its progressive dismantling.

Associated with the (North African) margin of Gondwana, the deposition of the Ediacaran Serie Negra Group has been traditionally considered as related to the opening of a peri-Gondwanan back-arc (Bandrés 2001). However, recent interpretations have also considered the possible deposition in a fore-arc basin opened during a short event of roll-back of the peri-Gondwanan trench that occurred at c. 600 Ma. The roll-back event favoured the generation of new oceanic lithosphere of supra-subduction zone type (Arenas et al. 2018; Díez Fernández et al. 2019). This new buoyant oceanic lithosphere was promptly obducted onto the magmatic arc as one of the ophiolites preserved in the Ossa–Morena Complex (Calzadilla Ophiolite). The major and trace element geochemistry, as well as the Nd isotopic data provided in this contribution for the Montemolín and Tentudía formations, are compatible with both (back- or fore-arc) tectonic settings affecting the thinned margin of Gondwana.

The constant highly negative $\varepsilon Nd_{(t)}$ values obtained for the Montemolín and Tentudía formations, constrained to a narrow interval ranging between −6.9 and −11.5, are paired to a relatively narrow interval of Paleoproterozoic Nd model ages ranging between 1686 and 1918 Ma. The limited variability of their Nd $T_{(DM)}$ model ages seems to indicate that they shared a common-source scenario for a long time. The detrital input derived from this source area remained essentially unchanged at least during the depositional time of the Montemolín and Tentudía formations, which ranges between c. 600 and 541 Ma. Altogether, these Nd model ages replicate the outcome obtained for the Serie Negra Group in the northern part of the Ossa–Morena Complex, in the Obejo-Valsequillo Domain (Rojo-Pérez et al. 2019).

The Nd model ages obtained for the Serie Negra Group representing the Cadomian basement in the SW Iberian Massif are almost identical to those obtained for coeval sedimentary series described in the Saxo-Thuringian Zone of the Bohemian Massif (Linnemann and Romer 2002). Their very similar T_{DM} values seem to indicate a common crustal provenance for the Ediacaran siliciclastic rocks that can be found along the Variscan Orogen, at least between SW Iberia and North Bohemia. A common provenance from old continental sources, previously located in the Gondwana mainland, is suggested by the highly negative values and the scarce variability obtained in the εNd range shown by these series. Nd model ages ranging between 2 and 1.6 Ga can only be obtained considering Paleoproterozoic and/or Archean sources, variably mixed with more juvenile material coming from the most external margin and/or the magmatic arc. An Ediacaran sedimentary basin located in the Gondwanan margin in front of the West African Craton, would probably account for the isotopic features recorded in the Ediacaran siliciclastic series from SW Iberia and North Bohemia (Fig. 9). This is in agreement with previous correlations suggested between both regions currently separated c. 2000 km (Fernández-Suarez et al. 2002; Linnemann et al. 2008; Pereira et al. 2015). The isotopic data considered in this contribution provide evidence about the correlation and peri-Gondwanan equivalence between the Cadomian basement of SW Iberia and North Bohemia. These data also indicate that both domains were located in a similar paleo-position in the African margin of Gondwana, although they could be separated from one another by a distance that must be shorter than the current one. Superimposed Variscan tectonics would have enlarged their primary distance by moving along strike the various tectonic blocks that make the Variscan Orogen. Consequently, the Ediacaran siliciclastic series located in SW Iberia and North Bohemia were probably deposited in a shared (long) sedimentary basin located in the Gondwana margin in front of the West African Craton, and whose length measured along the margin is yet to be constrained.

Acknowledgements Research funded by Spanish project CGL2016-76438-P (Ministerio de Economía, Industria y Competitividad). Reviews and constructive suggestions of the manuscript performed by Manuel Francisco Pereira and a second anonymous reviewer are gratefully acknowledged, as well as the important editorial work of Axel Gerdes.

Author contributions All authors have contributed actively in the creation of this manuscript.

Funding Research funded by Spanish project CGL2016-76438-P (Ministerio de Economía, Industria y Competitividad).

Availability of data and material All data utilized are included as tables and cited the sources.

Code availability Not applicable.

Compliance with ethical standards

Conflict of interest There are no conflicts of interest.

References

Abalos B (1987) Tectónica y metamorfismo en el Núcleo de Almadén de la Plata (Sevilla, Zona de Ossa–Morena). PhD Thesis. Universidad del País Vasco, pp 174

Abati J, Gerdes A, Fernández-Suárez J, Arenas R, Whitehouse MJ, Díez Fernández R (2010) Magmatism and early-Variscan continental subduction in the northern Gondwana margin recorded in zircons from the basal units of Galicia, NW Spain. Geol Soc Am Bull 122:219–235

Albert R, Arenas R, Gerdes A, Sánchez Martínez S, Fernández-Suárez J (2015) Provenance of the Variscan Upper Allochthon (Cabo Ortegal Complex, NW Iberia Massif). Gondwana Res 28:1434–1448

Allegre CJ, Rousseau D (1984) The growth of the continent through geological time studied by Nd isotope analysis of shales. Earth Planet Sci Lett 67:19–34

Alvaro JJ, Bellido F, Gasquet D, Pereira MF, Quesada C, Sanchez-Garcia T (2014) Diachronism in the Late Neoproterozoic-Cambrian arc-rift transition of North Gondwana: a comparison of Morocco and the Iberian Ossa-Morena Zone. J Afr Earth Sc 98:113–132

Andonaegui P, Arenas R, Albert R, Sánchez Martínez S, Díez Fernández R, Gerdes A (2016) The last stages of the Avalonian-Cadomian arc in NW Iberian Massif: isotopic and igneous record for a long-lived peri-Gondwanan magmatic arc. Tectonophysics 681:6–14

Arenas R, Sánchez Martínez S, Díez Fernández R, Gerdes A, Abati J, Fernández- Suárez J, Andonaegui P, González Cuadra P, López Carmona A, Albert R, Fuenlabrada JM, Rubio Pascual FJ (2016a) Allochthonous terranes involved in the Variscan suture of NW Iberia: a review of their origin and tectonothermal evolution. Earth Sci Rev 161:140–178

Arenas R, Díez Fernández R, Rubio Pascual FJ, Sánchez Martínez S, Martín Parra LM, Matas J, González del Tánago J, Jiménez-Díaz A, Fuenlabrada JM, Andonaegui P, García-Casco A (2016b) The Galicia–Ossa-Morena Zone: proposal for a new zone of the Iberian Massif. Variscan implications. Tectonophysics 681:135–143

Arenas R, Fernández-Suárez J, Montero P, Díez Fernández R, Andonaegui P, Sánchez Martínez S, Albert R, Fuenlabrada JM, Matas J, Martín Parra LM, Rubio Pascual FJ, Jiménez-Díaz A, Pereira MF (2018) The Calzadilla Ophiolite (SW Iberia) and the Ediacaran fore-arc evolution of the African margin of Gondwana. Gondwana Res 58:71–86

Avigad D, Gerdes A, Morag N, Bechstäd T (2012) Coupled U-Pb-Hf of detrital zircons of Cambrian sandstones from Morocco and Sardinia: implications for provenance and Precambrian crustal evolution of North Africa. Gondwana Res 21:690–703

Ballèvre M, Martínez Catalán JR, López-Carmona A, Pitra P, Abati J, Díez Fernández R, Ducassou C, Arenas R, Bosse V, Castiñeiras P, Fernández-Suárez J, Gómez Barreiro J, Paquette JL, Peucat JJ, Poujol M, Ruffet G, Sánchez Martínez S (2014) Correlation of the nappe stack in the Ibero-Armorican arc across the Bay of Biscay: a joint French-Spanish project. In: Schulmann K, Catalan JRM, Lardeaux JM, Janousek V, Oggiano G (eds) The Variscan Orogeny: extent, timescale and the formation of the European crust, vol 405. Geological Society of London, London, pp 77–113

Bandrés A (2001) Evolución geodinámica poliorogénica de los dominios septentrionales de la ZOM. PhD. Thesis. Universidad del País Vasco, pp 377

Bhatia MR (1983) Plate tectonics and geochemical composition of sandstones. J Geol 91:611–627

Bhatia MR, Crook KAW (1986) Trace elements characteristics of greywackes and tectonic setting discrimination of sedimentary basins. Contrib Miner Petrol 92:181–193

Brause H (1968) Das verdeckte Altpaliozoikum der Lausitz und seine regionale Stellung. Abh. Dtsch. Akad. Wiss., KI. Bergbau. Hiittenwes Montangeol 1:1–143

Carvalhosa A (1965) Contribuição para o conhecimento geológico da região entre Portel e Ficalho (Alentejo). Memorias dos Serviços Geológicos de Portugal. Nova Série 11:1–32

Casado BO (1998) Geochronological studies of the Pre-Mesozoic basement of the Iberian Massif: the Ossa Morena zone and the Allochthonous Complexes within the Central Iberian zone. PDd. Thesis. Swiss Federal Institute of Technology, Zürich, Switzerland, pp 235

Catalán JRM (2011) Are the oroclines of the Variscan belt related to late Variscan strike-slip tectonics? Terra Nova 23:241–247

Catalán JRM, Collett S, Schulmann K, Aleksandrowski P, Mazur S (2020) Correlation of allochthonous terranes and major tectonostratigraphic domains between NW Iberia and the Bohemian Massif, European Variscan belt. Int J Earth Sci 109:1105–1131

Condie KC (1993) Chemical composition and evolution of the upper continental crust: contrasting results from surface samples and shales. Chem Geol 104:1–37

Cullers RL (2002) Implications of elemental concentrations for provenance, redox conditions, and metamorphic studies of shales and limestones near Pueblo, CO, USA. Chem Geol 191:305–327

Dalziel IWD (1997) Overview: Neoproterozoic-Paleozoic geography and tectonics: review, hypotheses and environmental speculations. Geol Soc Am Bull 109:16–42

DePaolo DJ (1981) A neodymiun and strontium isotopic study of the Mesozoic calcalkaline granitic batholiths of the Sierra-Nevada and Peninsular ranges, California. J Geophys Res 86:470–488

Díez Fernández R, Arenas R (2015) The Late Devonian Variscan suture of the Iberian Massif: a correlation of high-pressure belts in NW and SW Iberia. Tectonophysics 654:96–100

Díez Fernández R, Martínez Catalán JR, Gerdes A, Abati J, Arenas R, Fernández-Suárez J (2010) U-Pb ages of detrital zircons from the basal allochthonous units of NW Iberia: Provenance and paleoposition on the northern margin of Gondwana during the Neoproterozoic and Paleozoic. Gondwana Res 18:385–399

Díez Fernández R, Arenas R, Pereira MF, Sánchez Martínez S, Albert R, Martín Parra LM, Rubio Pascual FJ, Matas J (2016) Tectonic evolution of Variscan Iberia: Gondwana–Laurussia collision revisited. Earth Sci Rev 162:269–292

Díez Fernández R, Jiménez-Díaz A, Arenas R, Pereira MF, Fernández-Suárez J (2019) Ediacaran obduction of a fore-arc ophiolite in SW Iberia: a turning point in the evolving geodynamic setting of peri-Gondwana. Tectonics 38:95–119

Eguíluz L (1988) Petrogénesis de rocas ígneas y metamórficas en el Antiforme Burguillos-Monesterio, Macizo Ibérico Meridional. PhD Thesis. Universidad del País Vasco, pp 694

Eguiluz L, Quesada C (1980) La sucesión Precámbrica de la transversal de Monesterio (Badajoz): Nota preliminar. Temas Geol Min 4:123–141

Eguíluz L, Abalos B, Ortega Cuesta LA (1990) Anfibolitas proterozoicas del sector central de la Zona de Ossa-Morena-geoquímica e implicaciones geodinámicas. Cuadernos do Laboratorio Xeológico de Laxe 15:119–131

Eguíluz L, Gil Ibarbuchi JI, Ábalos B, Apraiz A (2000) Superposed Hercynian and Cadomian orogenic cycles in the Ossa-Morena zone and related areas of the Iberian Massif. Geol Soc Am Bull 112:1398–1413

Fedo CM, Nesbitt HW, Young GM (1995) Unravelling the effects of potassium metasomatism in sedimentary rocks and paleosols, with implications for paleoweathering conditions and provenance. Geology 23:921–924

Feng R, Kerrich R (1990) Geochemistry of fine-grained clastic sediments in the Archean Abitibi greenstones belt, Canada: implications for provenance and tectonic setting. Geochim Cosmochim Acta 54:1061–1081

Fernández-Suarez J, Gutierrez-Alonso G, Jeffries TE (2002) The importance of along-margin terrane transport in northern Gondwana: insights from detrital zircon parentage in Neoproterozoic rocks from Iberia and Brittany. Earth Planet Sci Lett 204:75–88

Fernández-Suárez J, Arenas R, Abati J, Catalán JRM, Whitehouse MJ, Jeffries TE (2007) U-Pb chronometry of polymetamorphic high-pressure granulites: an example from the allochthonous terranes of the NW Iberian Variscan belt. In: Hatcher RD, Carlson MP, McBride JH, Catalán JRM (eds) 4-D framework of continental crust, vol 200. Geological Society of America, Boulder, pp 469–488

Fernández-Suárez J, Gutiérrez-Alonso G, Pastor-Galán D, Hofmann M, Murphy JB, Linnemanm U (2014) The Ediacaran-Early Cambrian detrital zircon record of NW Iberia: possible sources and paleogeographic constraints. Int J Earth Sci 103(5):1335–1357

Franke W (1989) Tectonostratigraphic units in the Variscan belt of central Europe. In: Dallmeyer RD (ed) Terranes in the Circum-Atlantic Paleozoic Orogens. Geological Society of America, Boulder, pp 67–90

Fricke W (1941) Die Geologie des Grenxebietes zwischen nordöstlicher Sierra Morena und Extremadura. PhD Thesis. University of Berlin, Berlin, Germany, pp 91

Fuenlabrada JM, Arenas R, Sánchez Martínez S, Díaz García F, Castiñeiras P (2010) A peri-Gondwanan arc in NW Iberia. I: isotopic and geochemical constraints on the origin of the arc-a sedimentary approach. Gondwana Res 17:338–351

Fuenlabrada JM, Pieren AP, Díez Fernández R, Sánchez Martínez S, Arenas R (2016) Geochemistry of the Ediacaran-Early Cambrian transition in Central Iberia: Tectonic setting and isotopic sources. Tectonophysics 681:15–30

Fuenlabrada JM, Arenas R, Sánchez Martínez S, Fernández RD, Pieren AP, Pereira MF, Chichorro M, Silva JB (2020) Geochemical and isotopic (Sm-Nd) provenance of Ediacaran-Cambrian metasedimentary series from the Iberian Massif. Paleoreconstruction of the North Gondwana margin. Earth Sci Rev. https://doi.org/10.1016/j.earscirev.2019.103079

Herron MM (1988) Geochemical classification of terrigenous sands and shales from core or log data. J Sediment Petrol 58:820–829

IGME (2014) Mapa geológico de España y Portugal E:1.1000.000. Instituto Geológico y Minero de España, Madrid

Jacobsen SB, Wasserburg GJ (1980) Sm-Nd isotopic evolution of chondrites. Earth Planet Sci Lett 50:139–155

Kossmat F (1927) Gliederung des varistischen Gebirgsbaues. Abh Sächs Geol Landesamt 1:1–39

Liew TC, Hofmann AW (1988) Precambrian crustal components, plutonic association, plate environment of the Hercynian fold belt of central Europe: indications from a Nd and Sr isotopic study. Contrib Miner Petrol 98:129–138

Liñán E, Fernández-Carrasco J (1984) La Formación Torreárboles y la paleogeografía del límite Precámbrico-Cámbrico en Ossa-Morena (Flanco Norte de la alineación Olivenza-Monesterio). Cuadernos do Laboratorio Xeolóxico de Laxe 8:315–328

Linnemann U (2007) Ediacaran rocks from the Cadomian basement of the Saxo-Thuringian Zone (NE Bohemian Massif, Germany): age constraints, geotectonic setting and basin development. Geol Soc Lond Spec Publ 286:35–51

Linnemann U, Buschmann B (1995) Der Nachweis der cadomischen Diskordanz in einer Tiefenbohrung bei Gera und deren Bedeutung für das proterozoischpaläozoische Standardprofil im Schwarzburger Antiklinorium. Geowissenschaftliche Mitteilungen von Thüringen 3:1–11

Linnemann U, Romer RL (2002) The Cadomian Orogeny in Saxo-Thuringia, Germany: geochemical and Nd–Sr-Pb isotopic characterization of marginal basins with constraints to geotectonic setting and provenance. Tectonophysics 352:33–64

Linnemann U, Schauer M (1999) Die Entstehung der Elbezone vor dem Hintergrund der cadomischen und variszischen Geschichte des Saxothuringischen Terranes-Konsequenzen aus einer abgedeckten geologischen Karte. Zeitschrift für Geologische Wissenschaften 27:529–561

Linnemann U, Gehmlich M, Tichomirowa M, Buschmann B, Nasdala L, Jonas P, Lützner H, Bombach K (2000) From Cadomian subduction to Early Palaeozoic rifting: the evolution of Saxo-Thuringia at the margin of Gondwana in the light of single zircon geochronology and basin development (Central European Variscides, Germany). In: Franke W, Haak V, Oncken O, Tanner D (eds) Orogenic processes: quantification and modelling in the Variscan Belt, vol 179. Geological Society of London, London, pp 131–153

Linnemann U, McNaughton NJ, Romer RL, Gehmlich M, Drost K, Tonk C (2004) West African provenance for Saxo-Thuringia (Bohemian Massif): did Armorica ever leave pre-Pangean Gondwana?—U-Pb–SHRIMP zircon evidence and the Ndisotopic record. Int J Earth Sci 93:683–705

Linnemann U, Pereira MF, Jeffries TE, Drost K, Gerdes A (2008) Cadomian Orogeny and the opening of the Rheic Ocean: new insights in the diachrony of geotectonic processes constrained by LA-ICP-MS U-Pb zircon dating (Ossa-Morena and Saxo- Thuringian Zones, Iberian and Bohemian Massifs). Tectonophysics 461:21–43

Linnemann U, Romer RL, Gerdes A, Jeffries TE, Drost K, Ulrich J (2010a) The Cadomian orogeny in the Saxo-Thuringian zone. In: Linnemann U, Romer RL (eds) Pre-Mesozoic Geology of Saxo-Thuringia—from the Cadomian active margin to the Variscan orogeny. Schweizerbart, Stuttgart, pp 37–58

Linnemann U, Hofmann M, Romer RL, Gerdes A (2010b) Transitional stages between the Cadomian and Variscan orogenies: Basin development and tectono-magmatic evolution of the southern margin of the Rheic ocean in the Saxo-Thuringian zone (North Gondwana shelf). In: Linnemann U, Romer RL (eds) Pre-Mesozoic Geology of Saxo-Thuringia—from the Cadomian active margin to the Variscan orogeny. Schweizerbart, Stuttgart, pp 59–98

Linnemann U, Gerdes A, Hofmann M, Marko L (2014) The Cadomian Orogen: Neoproterozoic to Early Cambrian crustal growth and orogenic zoning along the periphery of the West African Craton—constraints from U-Pb zircon ages and Hf isotopes (Schwarzburg Antiform, Germany). Precambr Res 244:236–278

Linnemann U, Pieren Pidal A, Hofmann M, Drost K, Quesada C, Gerdes A, Marko L, Gärtner A, Zieger J, Ulrich J, Krause R, Horak J (2018) A ~ 565 Ma old glaciation in the Ediacaran of peri-Gondwanan West Africa. Int J Earth Sci 107:885–911

López-Guijarro R, Armendariz M, Quesada C, Fernández-Suárez J, Murphy JB, Pin C, Bellido F (2008) Ediacaran-Palaeozoic tectonic evolution of the Ossa Morena and Central Iberian zones (SW Iberia) as revealed by Sm–Nd isotope systematics. Tectonophysics 461:202–214

Lugmair GW, Marti K (1978) Lunar initial 143Nd/144Nd: differential evolution of the lunar crust and mantle. Earth Planet Sci Lett 39:349–357

Lugmair GW, Shimamura T, Lewis RS, Anders E (1983) Sm-146 in the early solar system—evidence from neodymium in the Allende meteorite. Science 222:1015–1018

Matte PH (2001) The Variscan collage and orogeny (480–290 Ma) and the tectonic definition of the Armorica microplate: a review. Terra Nova 13:122–128

McCulloch MT, Wasserburg GJ (1978) Sm-Nd and Rb-Sr chronology of continental crust formation. Science 200:1003–1011

McLennan SM, Hemming SR (1992) Samarium/Neodymium elemental and isotopic systematics in sedimentary rocks. Geochimimica et Cosmochimica Acta 56:887–898

McLennan SM, Taylor SR, McCulloch MT, Maynard JB (1990) Geochemical and Nd–Srisotopic composition of deep-sea turbidites: crustal evolution and plate tectonic associations. Geochimimica et Cosmochimica Acta 54:2015–2050

Meert JG, Lieberman BS (2008) The Neoproterozoic assembly of Gondwana and its relationship to the Ediacaran-Cambrian radiation. Gondwana Res 14(5):21

Montero P, Salman K, Zinger T, Bea F (1999) Rb-Sr and single-zircon grain 207Pb/206Pb chronology of the Monesterio granodiorite and related migmatites. Evidence of Late Cambrian melting event in the Ossa-Morena Zone, Iberian Massif. Estudios Geológicos 55:3–8

Morag N, Avigad D, Gerdes A, Harlavan Y (2012) 1000–580 Ma crustal evolution in the northern Aranian-Nubian Shield revealed by U-Pb-Hf of detrital zircons from late Neoproterozoic sediments (Elat area, Israel). Precambr Res 208–211:197–212

Murphy JB, Eguiluz L, Zulauf G (2002) Cadomian orogens, peri-Gondwanan correlatives and Laurentia-Baltica connections. Tectonophysics 352:1–9

Nakamura N (1974) Determination of REE, Ba, Fe, Mg, Na and K in carbonaceous and ordinary chondrites. Geochim Cosmochim Acta 38:757–775

Nesbitt HW, Young GM (1982) Early Proterozoic climates and plate motions inferred from major element chemistry of lutites. Nature 299:715–717

Nesbitt HW, Markovics G, Price RC (1980) Chemical processes affecting alkalis and alkali earths during continental weathering. Geochim Cosmochim Acta 44:1659–1666

O'Nions RK, Carter SR, Evensen NM, Hamilton PJ (1979) Geochemical and cosmochemical applications of Nd isotope analysis. Annu Rev Earth Planet Sci 7:11–38

Pereira MF (2015) Potential sources of Ediacaran strata of Iberia: a review. Geodin Acta 27:1–14

Pereira MF, Chichorro M, Linnemann U, Eguiluz L, Silva JB (2006) Inherited arc signature in Ediacaran and Early Cambrian basins of the Ossa-Morena Zone (Iberian Massif, Portugal): paleogeographic link with European and North African correlatives. Precambr Res 144:297–315

Pereira MF, Chichorro M, Solá AR, Silva JB, Sánchez-García T, Bellido F (2011) Tracing the Cadomian magmatism with detrital/inherited zircon ages by in-situ U-Pb SHRIMP geochronology (Ossa-Morena Zone, SW Iberian Massif). Lithos 123:204–217

Pereira MF, Sola AR, Chichorro M, Lopes L, Gerdes A, Silva JB (2012a) North-Gondwana assembly, break-up and paleogeography: U-Pb isotope evidence from detrital and igneous zircons of Ediacaran and Cambrian rocks of SW Iberia. Gondwana Res 22:866–881

Pereira MF, Linnemann U, Hofmann M, Chichorro M, Solá AR, Medina J, Silva JB (2012b) The provenance of Late Ediacaran and Early Ordovician siliciclastic rocks in the Southwest Central Iberian Zone: constraints from detrital zircon data on northern Gondwana margin evolution during the late Neoproterozoic. Precambr Res 192:166–189

Perejón A, Liñán E, Quesada C (2004) Zona de Ossa-Morena. La evolución paleozoica. Sucesión preorogénica. Cámbrico. In: Vera JA (ed) Geología de España. SGE-IGME, Madrid, pp 1666–2169

Rodríguez-Alonso MD, Peinado M, López-Plaza M, Franco P, Carnicero A, Gonzálo JC (2004) Neoproterozoic-Cambrian synsedimentary magmatism in the Central Iberian Zone (Spain): geology, petrology and geodynamic significance. Int J Earth Sci 93:897–920

Rojo-Pérez E, Arenas R, Fuenlabrada JM, Sánchez Martínez S, Martín Parra LM, Matas J, Pieren AP, Díez Fernández R (2019) Contrasting isotopic sources (Sm-Nd) of Late Ediacaran series in the Iberian Massif: implications for the Central Iberian-Ossa Morena boundary. Precambr Res 324:194–207

Sánchez-García T, Bellido F, Quesada C (2003) Geodynamic setting and geochemical signatures of Cambrian-Ordovician rift-related igneous rocks (Ossa-Morena Zone, SW Iberia). Tectonophysics 365:233–255

Sánchez-García T, Pereira MF, Bellido F, Chichorro M, Silva JB, Valverde-Vaquero P, Pin C, Solá AR (2013) Early Cambrian granitoids of North Gondwana margin in the transition from a convergent setting to intra-continental rifting (Ossa-Morena Zone, SW Iberia). Int J Earth Sci 103:1203–1218

Sánchez-Lorda ME, Sarrionandia F, Ábalos B, Carracedo M, Eguiluz L, Gil-Ibarbuchi JI (2013) Geochemistry and paleotectonic setting of Ediacaran metabasites from the Ossa-Morena Zone (SW Iberia). Int J Earth Sci 103:1263–1286

Sánchez-Lorda ME, Ábalos B, García de Madinabeitia S, Eguiluz L, Gil Ibarguchi JI, Paquette JL (2016) Radiometric discrimination of pre-Variscan amphibolites in the Ediacaran Serie Negra (Ossa-Morena Zone, SW Iberia). Tectonophysics 681:31–45

Schäfer HJ, Gebauner D, Nägler TF, Eguiluz L (1993) Conventional and ion-microprobe U-Pb dating of detrital zircons of the Tentudia Group (Serie Negra, SW Spain): implications for zircon systematics, stratigraphy, tectonics and the Precambrian/Cambrian boundary. Contrib Miner Petrol 113:289–299

Stephan T, Kroner U, Romer RL (2019a) The pre-orogenic detrital zircon record of the Peri-Gondwanan crust. Geol Mag 156:281–307

Stephan T, Kroner U, Romer RL, Rösel D (2019b) From a bipartite Gondwana shelf to an arcuate Variscan belt: the early Paleozoic evolution of northern Peri-Gondwana. Earth Sci Rev 192:491–512

Stern RJ (2002) Crustal evolution in the East African Orogen: a neodymium isotopic perspective. J Afr Earth Sc 34:109–117

Taylor SR, McLennan SM (1985) The continental crust: its composition and evolution. Blackwell, Oxford, p 312

Thompson RN (1982) Magmatism of the British Tertiary province. Scott J Geol 18:49–107

Ugidos JM, Valladares MI, Barba P, Ellam RM (2003) The Upper Neoproterozoic-Lower Cambrian of the Central Iberian Zone, Spain: chemical and isotopic (Sm–Nd) evidence that the sedimentary succession records an inverted stratigraphy of its source. Geochim Cosmochim Acta 67:2615–2629

von Raumer JF, Stampfli GM (2008) The birth of the Rheic Ocean—Early Palaeozoic subsidence patterns and subsequent tectonic plate scenarios. Tectonophysics 461:9–20

von Raumer JF, Stampfli GM, Arenas R, Sánchez Martínez S (2015) Ediacaran to Cambrian oceanic rocks of the Gondwana margin and their tectonic interpretation. Int J Earth Sci 104:1107–1121

Winchester JA, Max MD (1989) Tectonic setting discrimination in clastic sequences: an example from the Late Proterozoic Erris Group, NW Ireland. Precambr Res 45:191–201

Wronkiewicz DJ, Condie KC (1987) Geochemistry of archean shales from the Witwatersrand supergroup, south Africa: source-area weathering and provenance. Geochim Cosmochim Acta 51:2401–2416

Zhao JX, McCulloch MT, Bennett VC (1992) Sm-Nd and U-Pb zircon isotopic constraints on the provenance of sediments from the Amadeus Basin, central Australia: evidence for REE fractionation. Geochim Cosmochim Acta 56(3):921–940